DESIGN AND ANALYSIS OF ADAPTIVE AND RECONFIGURABLE ANTENNAS FOR WIRELESS COMMUNICATION

by

MAHA ABDELMONEIM MOHAMED ALI
B.S. Ain Shams University, Cairo, Egypt, 1995
M.S. University of Central Florida, 1998

A dissertation submitted in partial fulfillment of the requirements
for the degree of Doctor of Philosophy
in the School of Electrical Engineering and Computer Science
in the College of Engineering and Computer Science
at the University of Central Florida
Orlando, Florida

Spring Term
2004

Major Professor: Parveen F. Wahid

ABSTRACT

Modern radar and communication systems have experienced a tremendous increase in the number of antennas onboard, on the ground, and in orbital space. This places a burden due to the confined volume and limited weight requirements especially in space applications. The reconfigurable antenna is a promising and exciting new type of antenna, where through the use of appropriate switches the antenna can be structurally reconfigured, to maintain the elements near their resonant dimensions for several frequency bands. This increases the bandwidth of the antenna dramatically, which enables the use of one antenna for several applications.

Four novel reconfigurable antenna elements were designed to work at 2.45 GHz and at 5.78 GHz, to cover the transition period when wireless communication will shift to the 5.78 GHz band. The four elements designed are: the reconfigurable Yagi, the reconfigurable corner-fed triangular loop antenna, the reconfigurable center-fed equilateral triangular loop antenna and the reconfigurable rectangular-spiral antenna. None of these antennas have been reported in the literature. Simulation results for all four antennas were obtained using IE3D. Fabrication and measurements for the Yagi antenna was done and the measured results agree with simulations. All four antennas have very good performance with respect to the 3dB beamwidth and directivity. However the reconfigurable rectangular-spiral antenna is the most compact in size among all four antennas. It is (20 mm x 20 mm) in size. At 2.45 GHz it has a 3dB beamwidth of

87^0 and directivity of 6.47dB. As for the 5.78GHz frequency the 3dB beamwidth is 82.5^0 and the directivity is 7.16dB.

This dissertation also introduces the use of reconfigurable antenna elements in adaptive arrays. An adaptive array that can null interference and direct its main lobe to the desired signal while being reconfigurable to maintain functionality at several frequency bands has the potential to revolutionize wireless communications in the future. Through several examples, at both the design frequencies, it is shown that the reconfigurable and adaptive antenna arrays are successful in nulling noises incident on the array. These examples illustrate how reconfigurable elements and adaptive arrays can be combined very beneficially for use in wireless communication systems.

To

My Family

ACKNOWLEDGEMENTS

I would like thank Dr. Wahid for her guidance and support throughout this work. Special thanks go to Dr. DeLoach for his help, many fruitful discussions and for taking the time to read through and review this dissertation. Thanks to Dr. Georgiopoulos, Dr. Wu and Dr. Jones for serving on my dissertation committee. I would also like to acknowledge Anand Arumugham for conducting the fabrication and the measurement of the Yagi array. Thanks also go to Mohua Kar for all her help.

I can not thank my husband, Sherif El-Tawil enough for always giving me the motivation, the support and the encouragement to continue working on my Ph.D. His patience and unlimited help were the reason I was able to complete this work. A special thanks to my daughter, Yara and to my sons Kareem and Bassem for their patience and understanding despite their very young age. Special gratitude goes to my mother, Soheir Elsaee, and my father, Abdelmoneim Ali for believing in me and teaching me that no challenge is insurmountable. Thanks also to my sister, Hala and my brothers, Mohamed and Hisham and all my family in Egypt for enduring my absence and for their prayers and encouragement.

Above all I thank God; without his guidance and help none of this would have been possible.

TABLE OF CONTENTS

LIST OF FIGURES

CHAPTER 1: INTRODUCTION

Adaptive Array Antennas

Adaptive array antennas, also known as smart antennas, have the ability to automatically respond to an unknown interference environment by steering nulls and reducing sidelobe levels in the direction of the interference, while maintaining some desired signal beam characteristics. They consist usually of an array of antenna elements and an adaptive receiver-processor which adjusts its element weights toward some optimization of output signal-to-interference-plus-noise ratio (SINR) in accordance with selected control algorithms.

A system consisting of an antenna array and an adaptive processor can perform filtering both in the space and the frequency domains, thus reducing the sensitivity of the signal-receiving system to an interfering directional noise source.

The first type of smart antenna was the sidelobe canceler developed at GE in the late 1950's invented by Paul Howells [1]. A sidelobe canceler consists of loop with a main high gain antenna for receiving the desired signal and one or more auxiliary low gain antennas to cancel the jamming signals by placing deep nulls in the sidelobe of the main antenna where the jammer signal is incident. The outputs of the antennas are weighted and combined until the jamming

signal is eliminated. The auxiliary antenna gains are designed to approximate the average sidelobe level of the main antenna gain pattern. This means they amplify the jamming signal approximately to the same level as the main antenna. Thus when the low gain auxiliary antenna signal is subtracted from the main high gain antenna, the jamming signal is canceled while the desired signal is not affected. Combining several of these loops together in an array created the adaptive array.

The feedback process needed to calculate the weights was developed by Appelbaum in his classic report [2], where he presented the control-law theory, an algorithm that maximizes the signal to noise ratio (SNR). Widrow [3], at the same time, presented the least mean square (LMS) algorithm to control the weights of an adaptive RF antenna system. These two algorithms are actually similar in that both derive their adaptive weight adjustment control by sensing the correlation between element signals, i.e., on the basis of the covariance matrix of the set of system inputs, and both converge toward the optimum Wiener solution on the basis of the eigenvalues involved.

The LMS was further developed by Griffith [4] and Frost [5], with the result that one can maintain a chosen frequency characteristics for the array in a desired direction, while discriminating against noise coming from other directions. Riegler and Compton [6] verifed the performance of the array experimentally using a laboratory array system oriented toward

communication applications. Zham [7] presented a power equalization technique that was shown to permit acquisition of weak signals in the presence of strong jamming.

The maixmum signal-to-noise signal (MSN) algorithm was developed by Brennan and Reed [8]-[10]. Their group has made significant contributions to the theory of adaptive radar systems, particularly those involving simultaneous adaptivity in both the spatial domain and the temporal (Doppler filter) domain. They describe in [11] a method of adaptively controlling both the angular and Doppler response for an AMTI (airborne moving target indication) radar . This AMTI technique provided an adaptive platform motion compensation for clutter cancellation, compensation for scattering from aircraft structures near the antenna, and adaptive nulling of external interference sources. Three different methods of generating the adaptive weights for control of the angular/Doppler response are described and compared.

Widrow and McCool [12] compared the performance characteristics of three algorithms used in adjusting the parameters of adaptive systems: the differential (DSD) and least-mean-square (LMS) algorithms, both based on the method of steepest descent, and the linear random search (LRS) algorithm, based on a random search procedure derived from the Darwinian concept of "natural selection." Theoretical and experimental results proved the LMS to be superior followed by the DSD and then the LRS.

The adaptive nulling methods described above are rather expensive to implement because they have a receiver at every element in the array and require calibration of all the receivrs. Baird and Rassweiler [13] have examined phase-only weighting as a means of lowering the cost of null-steering adaptive arrays. This approach makes use of conventional phased array architecture and varies the phase shifters and attenuators to minimize the total output power of the array. Mathematical equations for optimal phase weighting were developed and reduced to a simplified computational form. Computer simulations and breadboard array measurements substantiate the mathematical development and indicate the practicality of the method.

Applebaum and Chapman [14] examined the problem of incidental cancellations of the desired signal returns due to radar sidelobe jamming, returns from extended clutter and/or strong targets combined with longer transmitted waveform. They have examined some techniques in which the adaptive processor can be constrained from responding to desired main lobe target returns while maintaining good cancellation of interference in the sidelobes. Time, frequency and angle domain techniques are discussed and examples are given to show the effects of these constraints.

In [15] Tako et al. present the concept of the adaptive system working on the principle of minimizing the output power under directional constraint. A detailed theoretical analysis is presented and verified through computer simulation experiments on this system.

White [16] introduced an adaptive preprocessing network placed ahead of the main adaptation circuits of an adaptive antenna to speed the convergence rate by resolving the input signals into their eigenvector components. He showed that the preprocessor also achieves an improvement in the signal to interference ratio.

Chapman [17] has examined partial adaptivity in large arrays. As opposed to full adaptive arrays where each element of the array is individually controlled adaptively, in a partially adaptive array the elements are controlled in groups or only certain elements called auxiliary elements are made controllable. The problem of configuring such large arrays to provide partial adaptivity is examined.

The experimental pattern behavior of a four-element adaptive array based on the steepest-descent feedback algorithm is described in [18] by Compton. The operational patterns are measured versus several parameters and performance characteristics of the array are described.

Griffiths [19] and Washburn et. al. [20] have demonstrated experimentally that the adaptive beamforming improves the SNR by 10 dB to 20 dB when compared to conventional beamforming algorithms.

In 1986 Shmidt developed the Multiple Signal Classification (MUSIC) algorithm , which provides asymptotically unbiased estimates of 1) number of incident wavefronts present, 2)

directions of arrival (DOA) (or emitter location), 3) strength and cross correlation among incident waveforms and 4) noise/interference strength [21]. The MUSIC algorithm provides asymptotically unbiased estimates of a general set of signal parameters approaching the Cramer-Rao bound. Shmidt and Frank [22] report on the performance of an experimental system based on the signal subspace approach to multiple signal direction finding (DF) and source parameter estimation.

The application of spectral estimation techniques in adaptive array antennas is investigated in [23]. These techniques provide considerable amount of additional useful information about the interference environment, which is beyond that ordinarily available in conventional adaptive arrays. Two conceptual application area examples for using such techniques are discussed; partially adaptive low sidelobe arrays, and fully adaptive tracking arrays. Examples discussed include "superresoultion" effects, relative power level determination, estimation of coherent sources, and tracking/ cataloging/ranking of sources.

Gupta and Ksienski [24] , [25] have shown that the performance of an adaptive antenna array is strongly affected by the electromagnetic characteristics of the antenna array, The mutual coupling effect was however ignored. They assumed that the elements of the receiving array are isolated sources that sample but do not reradiate the incident field and that the array is isolated from its surrounding. However in a practical situation the elements do have mutual coupling, which affects the overall performance. In [26] the authors studied the effect of mutual coupling

on adaptive array performance. They define the mutual coupling as the mutual impedance of two thin half-wavelength dipoles and demonstrated that the effects of mutual coupling are significant even for large interelement spacing. Their study is focused on Applebaum-type arrays and on LMS-arrays.

Adve and Sarkar [27] have investigated the effects of mutual coupling between the elements of an array on direct data domain algorithms. They found that the mutual coupling severely undermines the interference suppression capabilities of direct data domain algorithms. The method of moments (MoM) was used to evaluate the mutual coupling between the elements. The MOM admittance matrix was then used to eliminate the effects of the mutual coupling and it was shown that performance was improved when mutual coupling effects were eliminated.

Reconfigurable Antennas

Modern radar and communication systems have experienced a tremendous increase in the number of antennas onboard, on the ground and in orbital space. Modern ships, airplanes and spacecraft require several antennas for broadband communication, radar, direction finding etc. This causes a problem due to the limited volume and weight constraints, especially in space applications. In addition, demands on reducing antenna size have become more and more pressing in order to reduce payload costs. Therefore it becomes highly beneficial to develop antennas that cover multiple frequency bands and serve different functionalities while sharing the

same physical aperture without sacrificing performance. Recently, reconfigurable antennas have been introduced to address these needs. These antennas have variable aperture sizes which can be obtained through the use of appropriate switching mechanism, e.g. by using MEMS (microelectromechanical systems) or PIN switches. Thus one antenna could be used for several applications, which saves space, weight and money. This is a new concept with many promising applications.

In one of the early papers on reconfigurable antennas, Schaffner et al [28] describe RF MEMS switches. The switch is based on a suspended cantilever structure, which minimizes the effects of residual stress on the mechanical performances. Schaffner introduces some ideas to use this switch to reconfigure printed circuit dipole and slot elements for frequency tuning and beamsteering. The length of the dipole can be lengthened or shorted by closing or opening the MEMS switch allowing for a change in the operational frequency. An array of these reconfigurable dipoles could be used in beam steering. The MEMS switch can also be placed across a slot antenna element to change its resonant properties. He also introduces the use of the switch in a reflective flared-notch element. By placing several MEMS switches across the coplanar strip transmission line that feeds the broadband flared aperture, appropriate time delays can be introduced to allow beam steering.

K.C. Gupta et al [29] introduced the idea of a frequency-reconfigurable rectangular ring slot antenna fed by a single slotline. MEMS switches were used to reconfigure the ring as shown in Figure 1. The periphery of the outer loop determines the lower frequency.

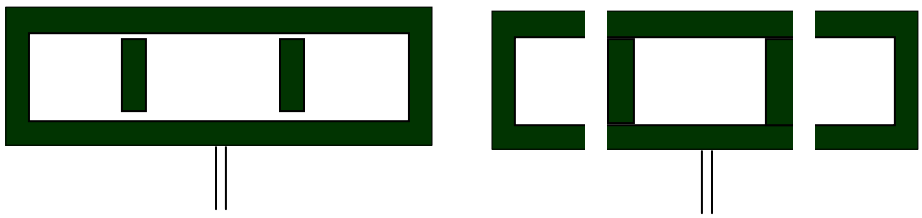

Figure 1: A single rectangular slot antenna reconfigured for operation at different frequencies by use of eight switches.

A reconfigurable aperture concept derived from fragmented aperture design is proposed by Maloney et al [30]. The reconfigurable aperture consists of a matrix of conducting patches with switches between some or all the patches. By opening or closing the switches functionality, like instantaneous bandwidth and steering angles can be changed.

Fathy et al [31] used the solid-state plasmas generated by PIN junctions to effectively implement various reconfigurable antennas. Injecting high dc currents into these PIN junctions in high resistivity silicon creates a plasma region with high conductivity. This defined metallic like

pattern can include the radiating element and the feeds as well. As an example they implemented a simple reconfigurable dipole to work in the 1-20GHz frequency range.

A new architecture for a MEMS reconfigurable VEE-antenna was designed and implemented by Chiao et al [32]. The planar Vee-antenna can be dynamically reconfigured for beam shaping and steering using electrically controlled micro-actuators. Theoretical and experimental beam patterns were investigated to demonstrate the beam steering and shaping capabilities of a 17.5 GHz MEMS Vee-antenna.

Elamaran et al [33] have investigated fixed frequency beam-steering arrays using reconfigurable periodic structures in the ground plane without solid-state phase shifters. Beam-steering is achieved by linearly varying the phase between adjacent elements of an antenna array using reconfigurable photonic band gaps (PBG) on ground plane. The experimental work was done using conducting tape to cover a number of selected PBG periods to obtain a discrete beam steering pattern. The beam steering angle varies linearly as the number of PBG periods is varied. A linearly discrete beam-steering of 35 degrees in steps of six degrees has been achieved at a fixed frequency of 5.6 GHz.

Weedon et. al [34] have investigated the design and fabrication of a dual L/X-band reconfigurable patch module (RPM) They used RT/duroid 5880 material with dielectric constant of 2.2 and loss tangent 0f 0.0009 at 10 GHz and they investigated the antenna for two different

thickness 0.062" and 0.125". The reconfigurable antenna was fabricated as two separate prototypes (open and closed configuration). They achieved 1.2% impedance bandwidth for the L-band configuration and greater than 7% bandwidth at X- band. The simulation results agreed well with the measurements.

VanBlaricum [35], presents the history of using photonic controlled switches in antenna design, which have been used mainly in the development of link and beam steering techniques. VanBlaricum also highlights the advantages of using photonically controlled switches in reconfigurable antennas.

Brown [36] discusses the first theoretical analysis on reconfigurable antennas. He conducts a full-wave analysis based on the method of moments on a reconfigurable-aperture antenna consisting of a two-dimensional array of filamentary microstrip dipoles interconnected by lossy MEMS switches. His primary purpose was to analyze the gain and impedance characteristics of a reconfigurable antenna and to compare them to those of a fixed-element antenna having identical architecture and material properties but lacking reconfigurabilty. A two-dimensional planar microstrip dipole array was analyzed varying the frequency between 16 and 2 GHz in octave increments. Two different array structures were considered. One a fixed-element aperture in which the dipole length is constant $d \approx \lambda_0/2\sqrt{\varepsilon_{eff}}$ at the maximum frequency of 16 GHz and the other a reconfigurable antenna in which the dipole length is maintained near $\lambda_0/2$ over several octaves of bandwidth via MEMS switches. In contrast to the fixed-element antenna, it was

shown that the reconfigurable antenna maintains a high gain with reduced frequency because its dipole lengths are maintained near the resonant length.

Adaptive and Reconfigurable Antennas

The combination of the advantages of both reconfigurability and adaptivity in a single antenna array has not yet been reported in the literature. It is our goal to pursue this task. An antenna that can null interference and steer its main beam towards desired signal and at the same time be reconfigurable to maintain functionality at several frequency bands is of great demand. In Chapter 2 adaptive array antennas are studied and the effect of mutual coupling is examined closely using the MoM. In Chapter 3 four novel reconfigurable antenna elements are introduced: The reconfigurable Yagi array antenna, the reconfigurable corner-fed equilateral triangle antenna, the center-fed equilateral triangle antenna and the reconfigurable rectangular-spiral antenna. None of these antennas have been reported before in the literature. They are designed to work in the transition period when wireless communication will shift to the higher 5.78 GHz band. In Chapter 4 we introduce the first antenna array of its kind, which is the adaptive and reconfigurable antenna array. Several examples show the feasibility of this idea. Chapter 5 includes conclusion and future work.

CHAPTER 2: ADAPTIVE ARRAY ANTENNAS

Introduction

Adaptive array antennas have the ability to automatically respond to an unknown interference environment by steering nulls and reducing sidelobe levels in the direction of the interference, while maintaining some desired signal beam characteristics. As shown in Figure 2, they consist usually of an array of antenna elements and an adaptive receiver-processor which adjusts its element weights toward some optimization of output signal-to-interference-plus-noise ratio (SINR). A system consisting of an antenna array and an adaptive processor can perform filtering both in the space and the frequency domains, thus reducing the sensitivity of the signal-receiving system to interfering directional noise source.

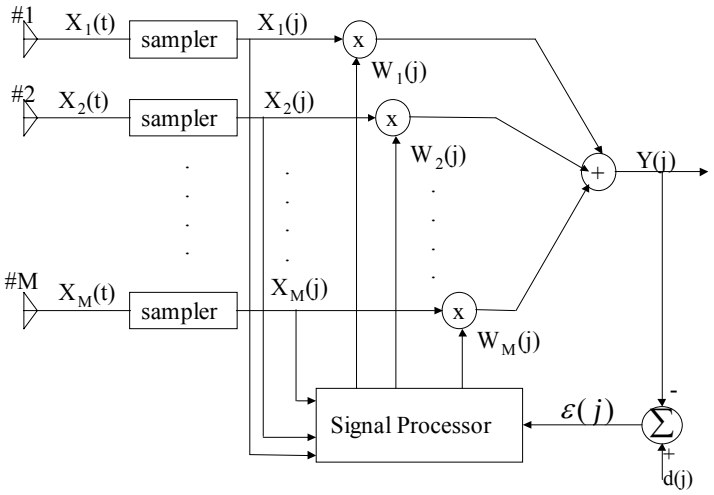

Figure 2: Adaptive array configuration

It has been shown [3], [24], [25] that the performance of an adaptive antenna array is strongly affected by the electromagnetic characteristics of the array. An important electromagnetic characteristic, namely the mutual coupling between the antenna element, has however been ignored. Mutual coupling becomes particularly significant as the interelement spacing is decreased.

In [26], it was shown that the mutual coupling between the elements of an adaptive array causes significant degradation in the signal-to-interference-plus-noise ratio and that it also slows the response of the array. These effects are significant even for large interelement spacing, i.e. for spacing more than half a wavelength. In [26] the mutual coupling effect was calculated by considering the N-element array as an N+1 terminal linear, bilateral network responding to an

outside source. Results show an improved performance of the adaptive array when the mutual coupling was accounted for and then eliminated.

In this chapter the method of moments (MOM) will be used to model the mutual coupling for signals arriving from a given direction of arrival (DOA) and to try to eliminate its effect by proper adjustment of the element weights. As a specific example, the method of moments will be used to analyze the response of a linear array of M thin, parallel, equispaced, identical wires, to an arbitrary incident field. The integral equation to solve for the unknown currents will be derived. This equation will then be approximately solved by dividing each wire into N subsections and using suitable basis functions and weighting functions, to convert the integral equation into a matrix equation. This matrix equation will then be solved to obtain the unknown currents.

The LMS Algorithm

The variable weights of a signal processor can be automatically adjusted by a simple adaptive technique based on the least-mean-square (LMS) algorithm. During the adaptive process an injected pilot signal simulates a received signal from a desired look direction. This allows the array to be trained so that its directivity pattern has a main lobe in the previously specified look direction. At the same time, the array processing system can reject any incident noises, whose direction of propagation are different from the desired look direction, by forming appropriate

nulls in the antenna directivity pattern. The array adapts itself to form a main lobe, with its direction and bandwidth determined by the pilot signal, and reject signals or noises occurring outside the main lobe as well as possible in the minimum mean square sense.

The output signal Y(j) in Figure 2 is the weighted sum displayed in Equation 2.1.

$$y(j) = \sum_{i=1}^{n} x_i(j) w_i \tag{2. 1}$$

where n is the number of weights and j indicates the jth sampling instant. This can be written in vector notation as:

$$y(j) = W^T X(j) \tag{2. 2}$$

where T denotes transpose and

$$W = \begin{bmatrix} w_1 \\ . \\ . \\ w_i \\ . \\ . \\ w_n \end{bmatrix} \tag{2. 3}$$

$$X(j) = \begin{bmatrix} x_1(j) \\ . \\ . \\ x_i(j) \\ . \\ . \\ x_n(j) \end{bmatrix} \tag{2. 4}$$

The difference between the desired response and the output response is the error signal ε(j) and is defined as:

$$\varepsilon(j) = d(j) - W^T X(j) \tag{2. 5}$$

The purpose of the adaptation or weight changing procedure is to find a set of weights that will adjust the output response of the adaptive element at each instant of time to be equal to or as close as possible to the desired response. In other words for each input vector X(j), the error ε(j) should be made as small as possible. A number of weight-adjustment procedures or algorithms exist which minimize the mean-square error. Minimization is usually accomplished by gradient-search techniques. One of those methods is the LMS algorithm. This algorithm is based on the method of steepest descent. Changes in the weight vector are made along the direction of the estimated gradient vector. Using this algorithm, the weight-adaptation formula is given by [3]

$$W(j+1) = W(j) - 2k_s \varepsilon(j) X(j) \tag{2. 6}$$

where

W(j) = weight vector before adaptation

W(j+1) = weight vector after adaptation

k_s = scalar constant controlling rate of convergence and stability ($k_s<0$)

Theory and Derivation

In this section the integral equation of thin wire antennas will be derived and solved using the moment method. The result will then be used to calculate the mutual coupling for an array of parallel thin wire antennas.

Derivation of the Integral Equation

A field incident on the surface S of an antenna or scatterer induces an electric current density $\vec{J_s}$ which in turn radiates the scattered field. If $\vec{J_s}$ is known, the scattered field everywhere that is due to $\vec{J_s}$ can be found using:

$$\vec{E}^s = -jw\vec{A} - \nabla\Phi \qquad (2.7)$$

where $\vec{A}$ is the magnetic vector potential, defined in Equation (2.8) and ϕ is the scalar potential and is given in Equation (2.9).

$$\vec{A} = \mu \oiint_{s} \vec{J}_s \frac{e^{-jkR}}{4\pi R} \tag{2. 8}$$

$$\Phi = \nabla \cdot \vec{A} \tag{2. 9}$$

For a thin wire antenna we can make the following approximations [37]

1. The current is assumed to flow only in the direction of the wire axis.
2. The current density is approximated by a filament of current I on the wire axis.
3. The boundary condition is applied only to the axial component of E at the wire surface.

So, assuming the wire antenna is parallel to the z-axis the above equations become:

$$E^s = -j\omega A_z - \frac{\partial \Phi}{\partial z} \tag{2. 10}$$

$$A_z = \mu \int_{axis} I(z') \frac{e^{-jkR}}{4\pi R} dz' \tag{2. 11}$$

$$\Phi = -\frac{1}{j\omega\varepsilon_0} \frac{\partial A_z}{\partial z} \tag{2. 12}$$

Taking the derivative of the above equation and substituting in the scattered field equation we get

$$E_z^s(r) = -j\frac{1}{\omega\mu\varepsilon_0}(k^2 A_z + \frac{\partial^2 A_z}{\partial z^2}) \tag{2. 13}$$

The z-component of the scattered field at the surface of the wire with length l is[38]

$$E_z^s(r=a) = -j\frac{1}{\omega\varepsilon_0}(k^2 + \frac{\partial^2}{\partial z^2})\int_{-l/2}^{l/2} I_z(z')\frac{e^{-jkR}}{4\pi R}dz' \tag{2. 14}$$

Applying the boundary condition that the total electric field at the wire vanishes at the wire surface,

$$E_z^t(r=a) = E_z^i(r=a) + E_z^s(r=a) = 0 \tag{2. 15}$$

Thus

$$E_z^i(r=a) = -E_z^s(r=a) \tag{2. 16}$$

Substituting this in the above equation and interchanging integration with differentiation, we can write

$$-j\omega\varepsilon E_z^i(r=a) = \int_{-l/2}^{l/2} I_z(z')\left[(k^2 + \frac{\partial^2}{\partial z^2})\frac{e^{-jkR}}{4\pi R}\right]dz' \tag{2. 17}$$

This equation is called Pocklington's integral equation. It can be expressed in a more convenient form as [39]

$$-E_z^i(r=a) = \frac{1}{j\omega\varepsilon}\int_{-l/2}^{l/2} I_z(z')\frac{e^{-jkR}}{4\pi\cdot R^5}\left[(1+jkR)(2\cdot R^2 - 3\cdot a^2) + (kaR)^2\right]dz' \tag{2. 18}$$

where R for observation points on the same wire is

$$R = \sqrt{a^2 + (z-z')^2} \tag{2. 19}$$

For observation points on the other antenna element of the array R becomes:

$$R \approx \sqrt{d^2 + (z-z')^2} \tag{2. 20}$$

where d is the distance between the array elements and a is replaced by d in the final form of Pocklington's equation given above.

Method of Moments

Pocklington integral equation relates the unknown total axial current I(z') on the wire to the known incident electric field. This equation is solved using the method of moments. To solve for the unknown current I(z') the wire of length L is divided into n subintervals of length $\Delta=l/n$ as shown in Figure 3. I(z') is then represented by a linear combination of known elements $g_n(z')$ of a basis set $\{ g_n(z') \}$ selected to approximate the current as

$$I(z') = \sum_n I_n g_n(z') \qquad (2.\ 21)$$

where I_n are the unknown coefficients.

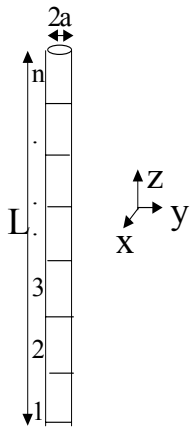

Figure 3 n segments on the wire antenna

Here, Galerkin's method is used, in which both the basis and weighting functions are set equal, i.e. $g_n = w_n$. Piecewise sinusoidal subdomain functions are selected as the basis functions giving

$$g_n(z') = \begin{cases} \dfrac{\sin[k(z'-z'_{n-1})]}{\sin[k\Delta]} & z'_{n-1} \le z' \le z'_n \\ \dfrac{\sin[k(z'_{n+1}-z')]}{\sin[k\Delta]} & z'_n \le z' \le z'_{n+1} \\ 0 & \textit{elsewhere} \end{cases} \qquad (2.\ 22)$$

where

$$\Delta = l/n = z'_{n+1} - z'_n \qquad (2.\ 23)$$

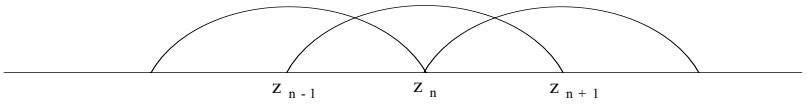

Figure 4: Piecewise sinusoidal subdomain basis function

With I(z') in the integral equation replaced by its approximation, Pocklington's equation becomes

$$-j\omega\varepsilon E_z^i(r=a) = \sum_n I_n \int_{-\frac{l_n}{2}}^{\frac{l_n}{2}} g_n(z') \frac{e^{-jkR}}{4\pi \cdot R^5} \left[(1+jkR)(2 \cdot R^2 - 3 \cdot a^2) + (kaR)^2 \right] dz' \qquad (2.24)$$

This gives one equation in n unknowns. To solve this equation we apply the method of weighted residual. We define the residual "Res" to be the sum of the tangential components of the scattered and incident fields

$$\mathrm{Re}\,s = E_z^i(r=a) + E_z^s(r=a) \qquad (2.25)$$

$$\mathrm{Re}\,s = \sum_n I_n \int_{-\frac{l_n}{2}}^{\frac{l_n}{2}} g_n(z') \frac{e^{-jkR}}{4\pi \cdot R^5}\left[(1+jkR)(2\cdot R^2 - 3\cdot a^2) + (kaR)^2\right]dz' + j\omega\varepsilon E_z^i(r=a) \tag{2.26}$$

Clearly we want this residual to be zero. In the method of weighted residuals the I_n's are found such that the residual is forced to zero in a weighted average sense. So we choose n-weighting or testing functions, such that

$$\int_{-l/2}^{l/2} W.\mathrm{Re}\,s = 0 \tag{2.27}$$

We define a set of weighting functions $w_m(z)$ on each subinterval as

$$\int_{-l/2}^{l/2} w_m(z) \sum_n I_n \int_{-\frac{l_n}{2}}^{\frac{l_n}{2}} g_n(z') \frac{e^{-jkR}}{4\pi \cdot R^5}\left[(1+jkR)(2\cdot R^2 - 3\cdot a^2) + (kaR)^2\right]dz'dz + \int_{-l/2}^{l/2} w_m(z)\, j\omega\varepsilon E_z^i(z)dz = 0 \tag{2.28}$$

and interchanging summation with integration we have

$$\sum_{n} \int_{-\frac{l_m}{2}}^{\frac{l_m}{2}} w_m(z) I_n \int_{-\frac{l_n}{2}}^{\frac{l_n}{2}} g_n(z') \frac{e^{-jkR}}{4\pi \cdot R^5} \left[(1 + jkR)(2 \cdot R^2 - 3 \cdot a^2) + (kaR)^2 \right] dz' dz + \int_{-l_m/2}^{l_m/2} w_m(z)\, j\omega\varepsilon E_z^i(z) dz = 0 \qquad (2.\ 29)$$

We now have n equations in n unknowns. This equation can be written in matrix form as:

$$[V_m] = [Z_{mn}]\ [I_n] \qquad (2.\ 30)$$

where

$$V_m = - \int_{-l_m/2}^{l_m/2} w_m(z)\, j\omega\varepsilon E_z^i(z) dz \qquad (2.\ 31)$$

$$Z_{mn} = \sum_{n} \int_{-\frac{l_m}{2}}^{\frac{l_m}{2}} w_m(z) I_n \int_{-\frac{l_n}{2}}^{\frac{l_n}{2}} g_n(z') \frac{e^{-jkR}}{4\pi \cdot R^5} \left[(1 + jkR)(2 \cdot R^2 - 3 \cdot a^2) + (kaR)^2 \right] dz' dz \qquad (2.\ 32)$$

This matrix equation can now be solved for the unknown coefficients I_n through matrix inversion as follows

$$\left[I_n\right] = [Ymn][Vm] \tag{2. 33}$$

where [Ymn] is the MOM admittance matrix of order n × n , where as mentioned above, n is number of sections in the wire. $[I_n]$ and $[V_m]$ are column matrices of order n and m respectively.

This procedure can be easily extended to calculate the current for an array of M wires as shown in Figure 5

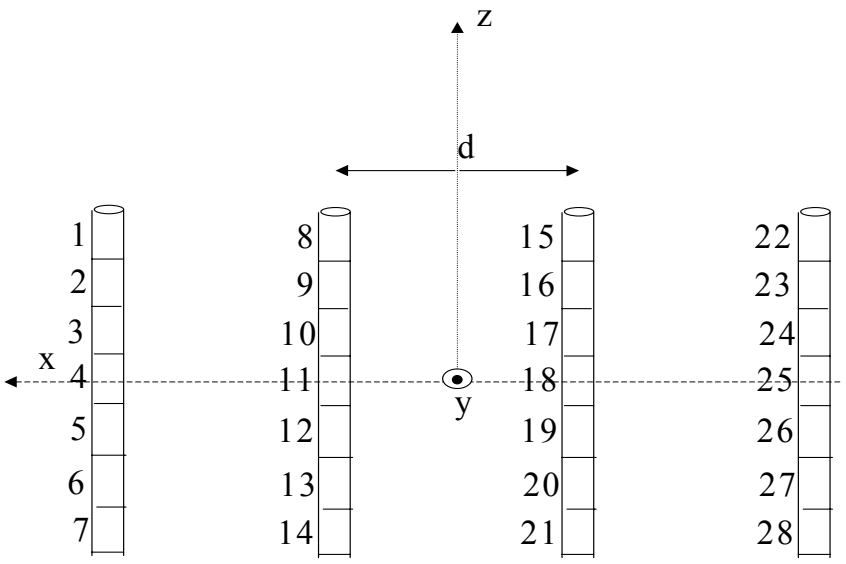

Figure 5 Array of M parallel wire antenna

The above equation can be written as

$$\left[I_{MOM}\right] = [Y_{MOM}][V_{MOM}] \tag{2. 34}$$

In this equation $[Y_{MOM}]$ is of order N × N, where N is the total number of unknowns in the MOM solution. In other words N = n × M , where M is the total number of array elements and n is the number of subsections in each wire. The admittance matrix $[Y_{MOM}]$ contains all the information about the mutual coupling between the elements of the array.

Elimination of the Mutual Coupling Effect in Adaptive Array Antennas

In this section, the method proposed in [40] to eliminate the effect of mutual coupling is presented and implemented in a two element dipole array.

The voltages measured at the ports of the array are related to the currents at the ports by

$$[V_{meas}] = [Z_L]\,[I_{port}] \tag{2. 35}$$

where $[Z_L]$ is the diagonal load matrix, whose elements are usually chosen to be the complex conjugate of the self impedance of each array element. The entries in $[V_{meas}]$ correspond to the entries of [X] in the weight-adjustment formula of the LMS algorithm. These are the signals fed to the processor for weight adjustment. If the processor is not programmed to take the mutual coupling into account, the calculated weights will be erroneous, because V_{meas} is the actual

voltage measured at the ports and is affected by mutual coupling. Thus the array will not perform as expected.

The entries of [Iport] are just selected entries of $[I_{MOM}]$ that correspond to a port. Thus the above equation can be written as:

$$[V_{meas}] = [Z_L][Y1_{MOM}][V_{MOM}] \tag{2. 36}$$

where $[Y1_{MOM}]$ is an M×N matrix with only the rows of $[Y_{MOM}]$ that correspond to a port. Given the directional of arrival of the signal (θ,φ) and the fact that the entries of $[V_{MOM}]$ are directly related to the incident field, we can write

$$V_{MOM}^{q+p,m} = V_{MOM}^{q,m} e^{\pm jkp\Delta z\cos\theta} \tag{2. 37}$$

where Δz is the subsection length, k the wave-number, q the subsection number in wire number m. Thus we can write the equation for $[V_{meas}]$ as

$$[V_{meas}] = [Z_L][Y2][V_{inc}] \tag{2. 38}$$

where the M×N matrix of $[Y1_{MOM}]$ is reduced to a M×M matrix [Y2] by incorporating the exponential factor given above. $[V_{inc}]$ is the matrix with entries of $[V_{MOM}]$ that correspond to the

ports of the array. They correspond directly to the incident field. The voltages given in [Vinc] are free of mutual coupling for signals arriving from the given direction of arrival. Thus if the adaptive processor is programmed to solve for $[V_{inc}]$ using $[V_{meas}]$ as given in the above equation, and use $[V_{inc}]$ instead of $[V_{meas}]$ to adjust the weights, it will overcome the problem of mutual coupling. This is illustrated by an example in the next section.

Results

The equations derived above are implemented by computer codes written in C. One program computes the mutual coupling of the array and the measured voltage at the ports. Another program uses the measured voltage and adjusts the weights of the array elements, using the LMS algorithm, to get the desired response.

A simple example of a two element array was considered and implemented to test the method proposed above to eliminate mutual coupling in an adaptive array. In this example it was be assumed that the desired signal is arriving from the direction $\Phi = 0$ and the noise signal is incident on the receiving array at an angle $\Phi = \pi/6$. The array consists of a two half wavelength dipoles separated by distance $d = \lambda/2$ as shown Figure 6. Using the mutual coupling C- program, the voltage measured at the ports was computed for both the signal and noise. These voltages were then used to adjust the weights of the array to extract the desired signal and reject the noise using the LMS program.

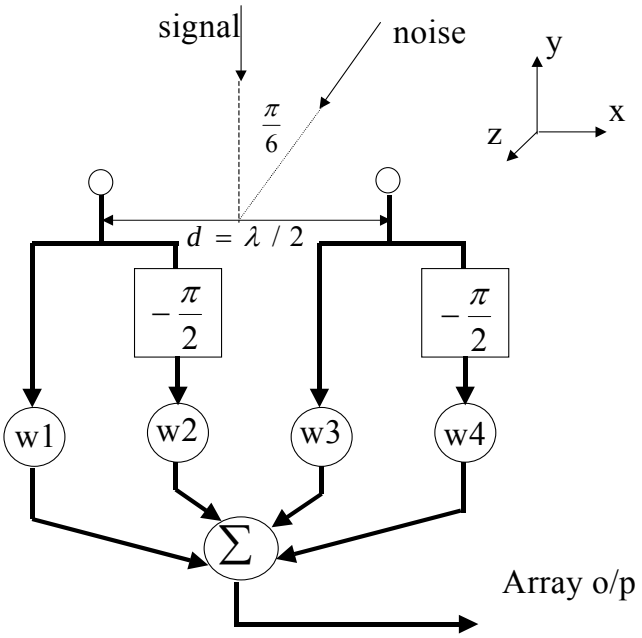

Figure 6: Array configuration for noise elimination example

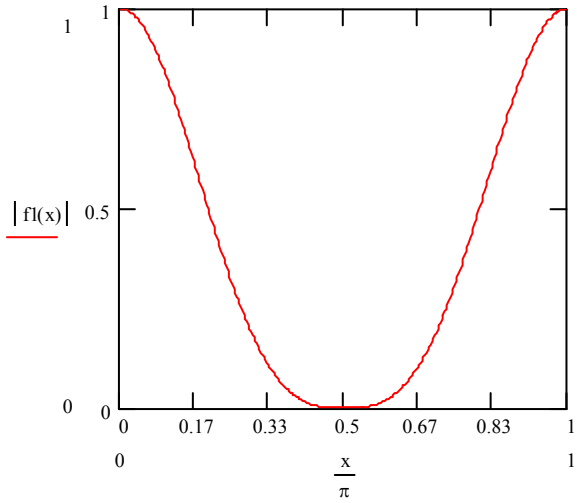

Figure 7: Directivity pattern of the non-adaptive two-element half wavelength dipole array.

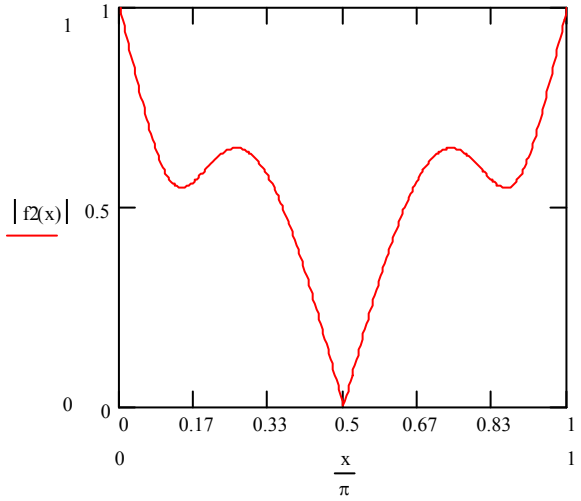

Figure 8: Directivity pattern of a two-element half wavelength adaptive dipole array with the effect of mutual coupling.

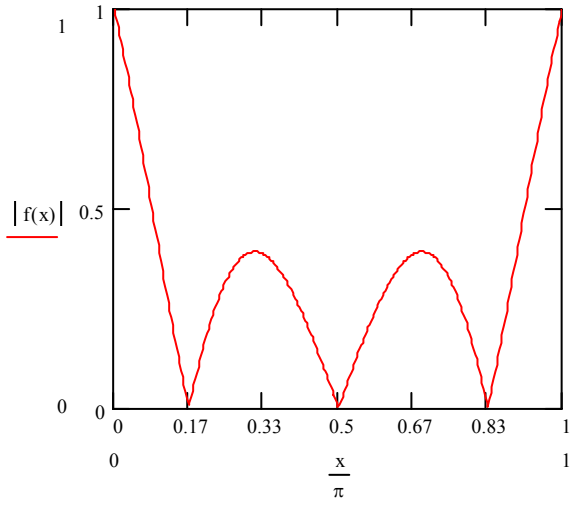

Figure 9 : Directivity pattern of two-element half wave length adaptive dipole array. The mutual coupling effect have been taken into account and eliminated.

Figure 7 shows the directivity pattern of a two-element half wavelength non-adaptive dipole array, i.e. in Figure 6 the weights, w1= w3=1 and w2 = w4 =0. When initially the weights are adaptively adjusted using the LMS algorithm to reject the noise incident at $\Phi = \pi/6$ without correcting for the mutual coupling effect, the results shown in Figure 8 are obtained. As can be seen, the noise has not been nulled completely. This will certainly degrade the performance of the array. Using the method described above [40] to eliminate the mutual coupling effects, we get the results of Figure 9. Now the noise at $\Phi = \pi/6$ has been successfully nulled out as desired.

Conclusion

In this chapter the mutual coupling effect on the behavior of adaptive array antennas was analyzed using the moment method. A C-program was developed to model the mutual coupling and the weights of the adaptive array were adjusted using a C-program based on the Least Mean Square algorithm. Through an example of a two-element half wavelength adaptive dipole array, it was shown that the mutual coupling between the elements of an adaptive array causes significant degradation in the performance of the array and thus should not be neglected. A method to eliminate the mutual coupling effect was presented and it was demonstrated that this algorithm successfully eliminates the effects of mutual coupling on adaptive arrays.

CHAPTER 3: RECONFIGURABLE ANTENNAS

Introduction

A reconfigurable antenna is a revolutionary new type of an antenna. Using MEMS switches, PIN switches, or other switching mechanisms, a reconfigurable antenna can be structurally reconfigured to operate at different frequency bands. Thus one antenna could be used for several applications, which saves space, weight and money. In this chapter, reconfigurable antennas are presented and their advantages are discussed. Four novel reconfigurable antennas, which have not been reported in the literature, are presented.

Reconfigurable Antennas

The distinguishing feature of a reconfigurable antenna is that it can alter the RF current distribution within a planar-radiating aperture. As opposed to a phased array it can change its element pattern in addition to its complex array factor. The far field from traditional-phased array can be written as displayed in Equation 3.1 [41]

$$\vec{E} = \frac{j\omega\mu_o}{4\pi}\frac{e^{-jkr_0}}{r_0} f_e(\theta,\phi) f_a(\theta,\phi) \tag{3.1}$$

where, $f_e(\theta,\phi)$ is the element factor and $f_a(\theta,\phi)$ is the array factor.

In traditional phased array antennas, the element factor is fixed by design and cannot be altered. The far field pattern is changed only by variation of the complex coefficients in the array factor. In a reconfigurable antenna the element factor can also be changed by altering the physical aperture of the antenna. Reconfigurable antennas with the antenna aperture controlled using PIN junctions [31,42] or using photonically controlled devices [35] have been reported. Many researchers have incorporated microelectromechanical (MEMS) switches in their antenna designs to attain reconfigurability with microstrip patch antennas [28,34,43].

In [36] it was shown that a reconfigurable array of resonant elements can maintain a high gain over a wide (reconfiguration) bandwidth by varying the element length and interelement separation such that they are maintained at or near resonance at each frequency. The performance of fixed-element aperture in which the dipole length was fixed at $d \approx \lambda_0/2(\varepsilon_{eff})^{0.5}$ at the maximum frequency of 16GHz was compared with a reconfigurable aperture array in which the dipole length is maintained near $\lambda_0/2$ over several octaves of bandwidth by judicious activation of MEMS switches between the elements. For the fixed element aperture, the gain and aperture efficiency was found to decrease rapidly with frequency because of a rapid increase in the return loss arising from impedance mismatch between the generators and dipole elements. In

contrast, for low MEMS switch insertion loss, the reconfigurable array maintains high gain with reduced frequency that nearly tracks the diffraction limit ($4\pi A/\lambda_0^2$). This is because the switches maintain the dipole length near the $\lambda_0/2$ resonance length.

Reconfigurable Antennas for Wireless LAN Communication

In general, antennas that can be used in wireless LAN communication applications should maintain certain specifications. The antenna size is very important. The antenna element should be compact enough to be placed, for example, on laptop computers or to fit on a PCS card. In addition the antenna should have a broad beam and nearly omni-directional coverage to be able to receive signals from any direction the user desires.

In wireless communications applications reconfigurability of the antennas used will instill extreme advantages. For example, using switches the antenna can be reconfigured to receive video, audio, or internet signal. Four different reconfigurable elements, designed to work at both the 2.4GHz and the 5.78GHz frequencies, are presented here. They are intended to be used in the transition period where wireless communications shifts to the higher 5.78GHz frequency range.

Reconfigurable Yagi Array Antenna

A reconfigurable planar Yagi array was designed to work at both the 5.78 GHz and 2.4 GHz frequencies. The Yagi was designed using a basic reconfigurable dipole to work at the two frequencies with double the number of reflectors and directors at the higher frequency than the lower one. Using a reconfigurable antenna element in an array requires adjusting the distance between the elements to operate at the different frequency bands. Figure 10 shows the reconfigurable Yagi with the switches in the open state where it operates at the higher frequency and Figure 11 shows it with the switches in the closed state where it operates at the lower frequency. Simulation results for this antenna were obtained using IE3D. Fabrication of the microstrip Yagi was done using RT Duroid 5880 with $\varepsilon_r = 2.2$ and a substrate thickness of 5 mils with no ground plane. The antenna was tested as two separate prototypes for the open and closed states of the switches to illustrate the feasibility of the design. In both simulation and measurement, the MEMS switches were considered ideal open/closed switches.

Figure 12 and Figure 13 show measured results compared to the simulation results obtained using IE3D. At the 2.4 GHz frequency the antenna has a 3db beamwidth of 57.6^0 and a directivity of 8.62 db. At 5.78 GHz the antenna has a 3db beamwidth of 37.4^0 and a directivity of 11.49 db.

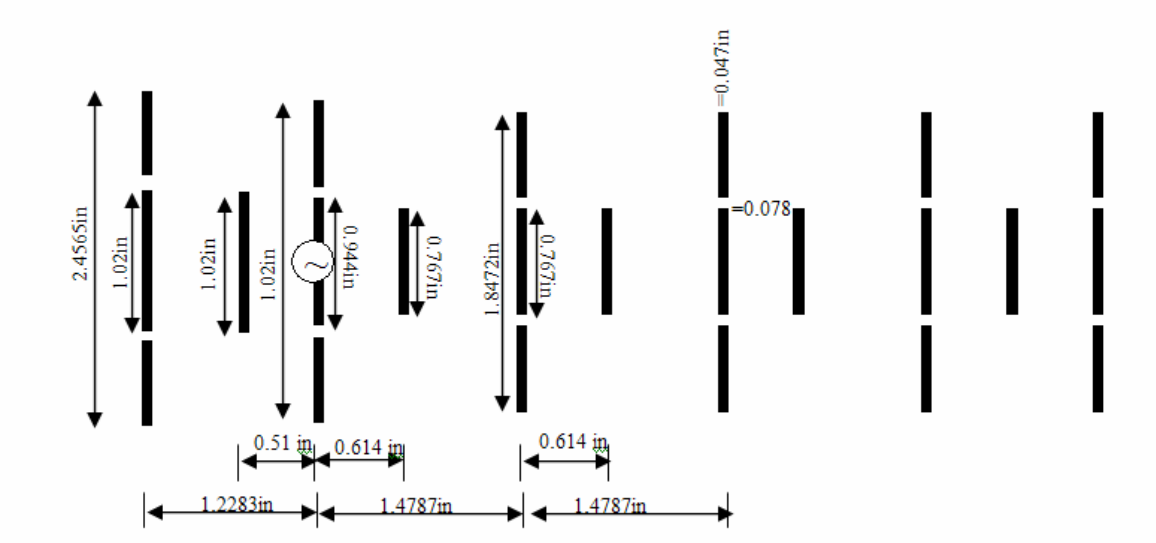

Figure 10: The reconfigurable Yagi array at 5.78 GHz, with the switches open.

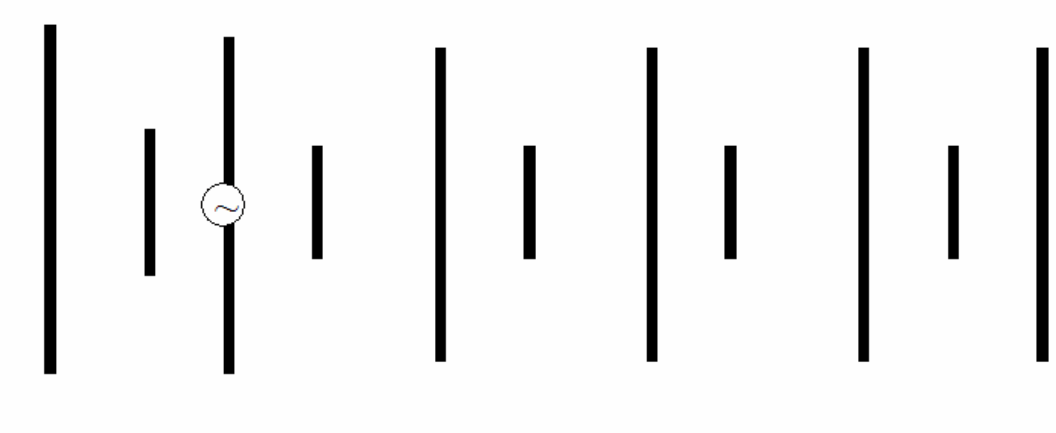

Figure 11: The reconfigurable Yagi array at 2.4 GHz, with the switches closed.

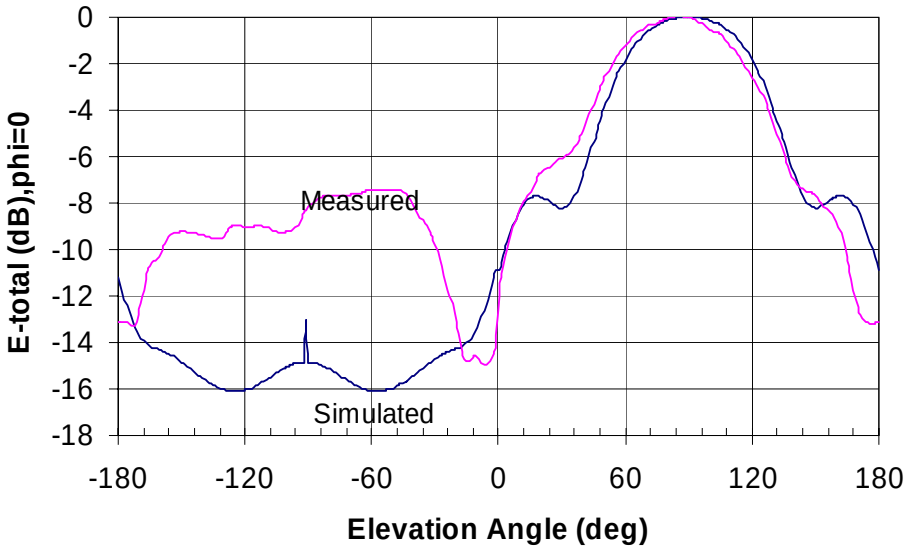

Figure 12: Simulated and measured radiation pattern, with the switches closed, f = 2.4GHz

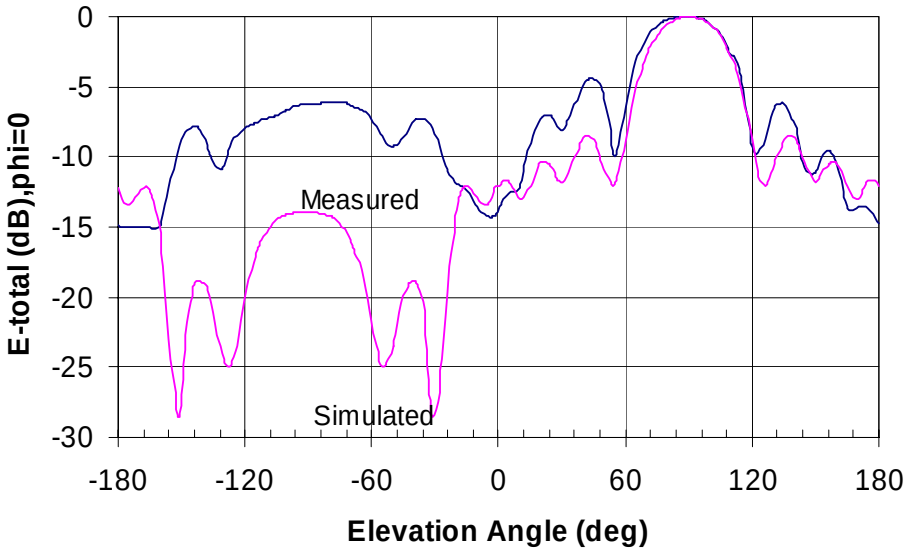

Figure 13: Simulated and measured radiation pattern, with the switches open, f = 5.78GHz

Reconfigurable Equilateral Triangular Loop Antenna

The reconfigurable Yagi antenna presented above with dimensions of (60mm X 175.01mm) can still be used on laptops for wireless LAN communication. Using it as an element in an array though, would make the array dimensions too big for practical application. In addition it uses 12 MEMS switches which will be expensive to manufacture and operate. This has led us to the design of other more compact reconfigurable elements. In this section, two types of the reconfigurable equilateral triangular loop antenna are presented, the corner-fed and the center-fed. In general loop antennas are designed with perimeter close to one wavelength at the operating frequencies to maintain good radiation pattern and input impedance. The equilateral triangular loop is chosen because of its smaller area size compared to the rectangular and circular loop with same perimeter and similar radiation characteristics at a given frequency. This makes it a good candidate for compact antenna design. Four switches are used to configure the antenna to operate at either the 2.45GHz or at 5.78GHz. Simulation results were again obtained using IE3D with the MEMS switches modeled as ideal open/closed switches. The substrate had ε_r=2.55 and thickness of 1.59mm. An infinite ground plane was assumed.

Reconfigurable Corner-fed Equilateral Triangular Loop Antenna

This antenna is fed in the corner of the triangle using a coaxial cable. Through four switches the antenna can be reconfigured to work at either 2.45GHz or at 5.78GHz. The reconfigurable

equilateral triangular loop antenna with all the four switches open is shown in Figure 14. The triangle perimeter is maintained near one wavelength for each of the operating frequencies. The side lengths for the two triangles are 40.8mm and 17.4 mm respectively. The bigger dimension equilateral triangle is designed for the 2.45GHz frequency, while the smaller one is for the 5.78GHz operation. Figure 15 shows the reconfigurable antenna with the appropriate switches closed for the 2.4GHz operation while Figure 16 shows the switches closed for the 5.78GHz frequency operation. Figure 17 and Figure 18 show the antenna polar elevation radiation pattern ($\varphi=0^{o}$) for both the 5.78GHz and 2.45GHz operating frequencies respectively, obtained through IE3D simulation. At 2.45GHz the antenna has a 3dB beamwidth of 78.6^{0} and a directivity of 8.07 dB. At 5.78GHz the 3dB beamwidth is 94^{0} and the directivity is 7.175 dB.

Compared to the reconfigurable Yagi antenna shown in Figure 10 with overall dimensions of (60mm X 175.01mm), the reconfigurable equilateral triangular loop antenna is clearly much more compact in size, uses smaller number of switches which makes it less expensive and has a broader beamwidth which makes it more suitable for wireless LAN communication.

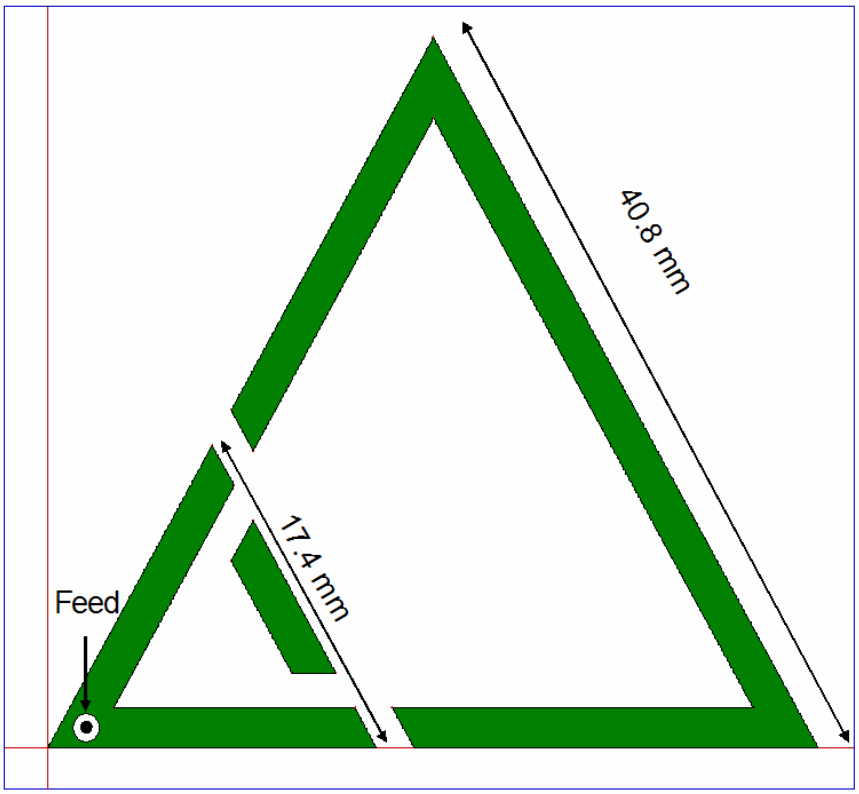

Figure 14 : The corner-fed reconfigurable equilateral triangular loop antenna with all the switches open.

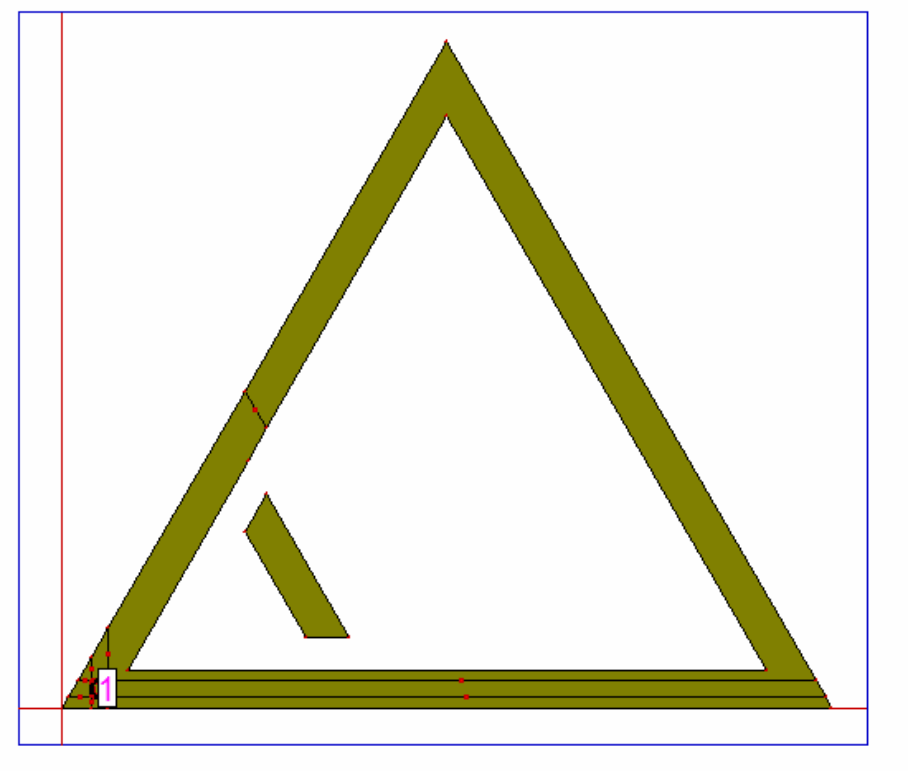

Figure 15: The reconfigurable equilateral triangular loop antenna with the switches closed for the 2.4GHz frequency operation

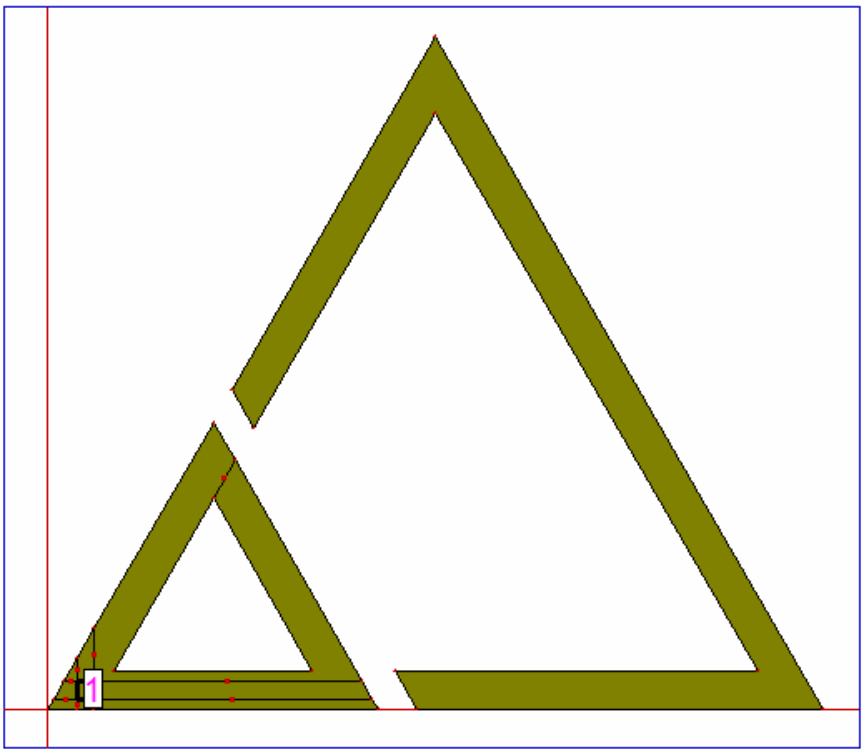

Figure 16: The reconfigurable equilateral triangular loop antenna with the switches closed for 5.78 GHz frequency operation

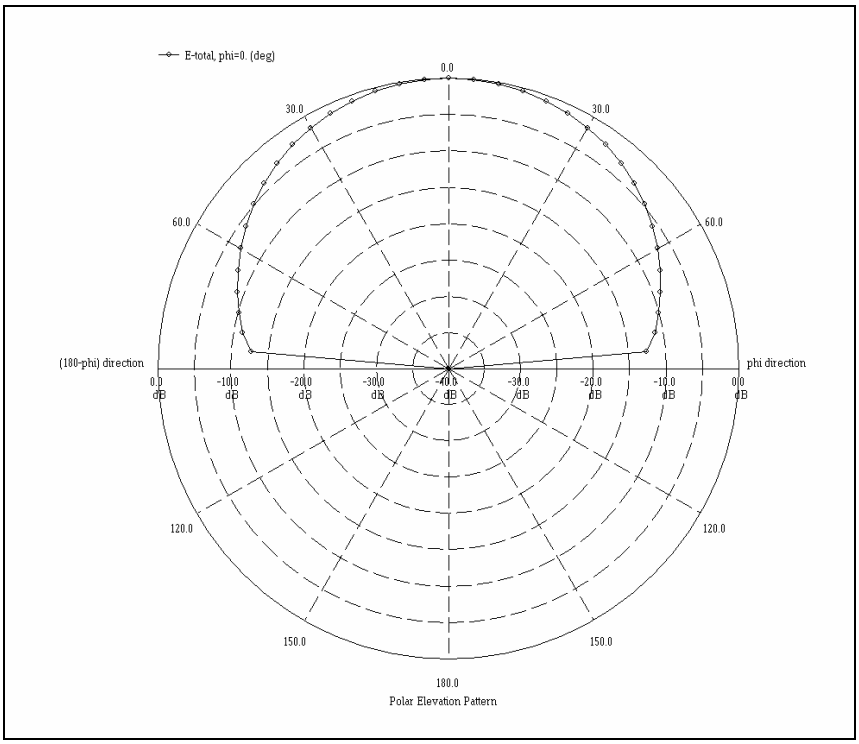

Figure 17 : Simulated radiation pattern in the elevation plane (φ=0º) for the reconfigurable corner-fed equilateral triangular loop antenna at 2.45GHz

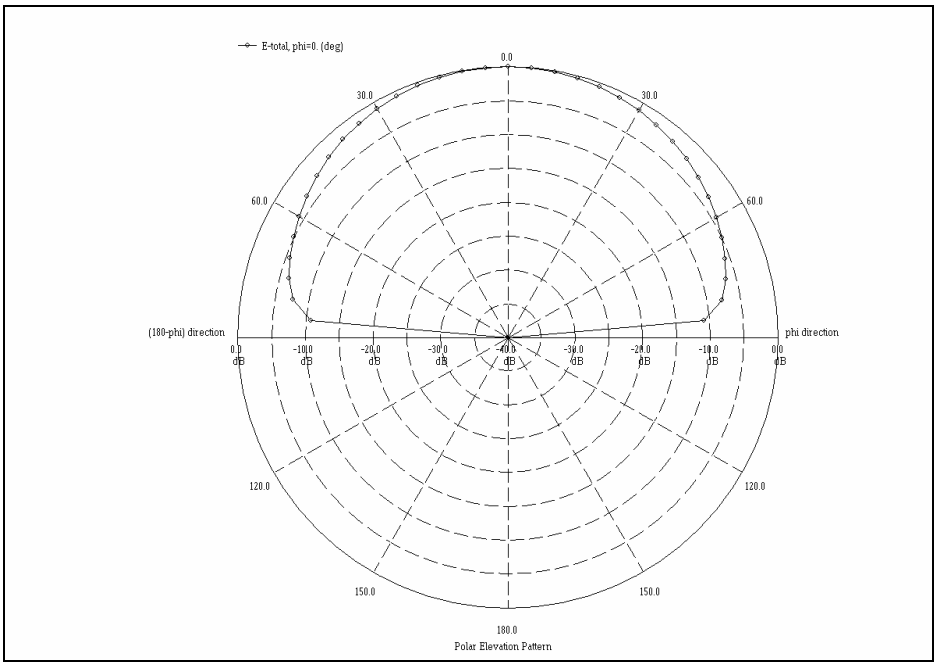

Figure 18: Simulated radiation pattern in the elevation plane (φ=0º) for the reconfigurable corner-fed equilateral triangular loop antenna at 5.78 GHz

Reconfigurable Center-fed Equilateral Triangle Loop Antenna

As a variation to the corner-fed equilateral triangular antenna presented above, the center-fed equilateral triangular loop antenna was designed. As shown in Figure 19, the coaxial line feeding this antenna is located in the center of its base for the two operating frequencies. With the same dimensions as the corner-fed type, this antenna is designed to work at the 2.45GHz and at the 5.78GHz frequencies. It also uses 4 MEMS switches for reconfiguration. Figure 20 and Figure 21 show the switching for each frequency respectively. IE3D simulation results of the

radiation pattern are shown in Figure 22 for the 2.45GHz and in Figure 23 for the 5.78GHZ frequency. The antenna has 3dB beamwidth of 89.25^0 and directivity of 7.1 dB at the 2.45 GHz operating frequency. For the 5.78GHz configuration it has 94.7º beamwidth and the directivity is 6.8 dB.

As compared to the corner-fed reconfigurable equilateral triangular loop, the center-fed element has a similar radiation pattern with a slightly wider beamwidth making it more suitable for wireless LAN applications.

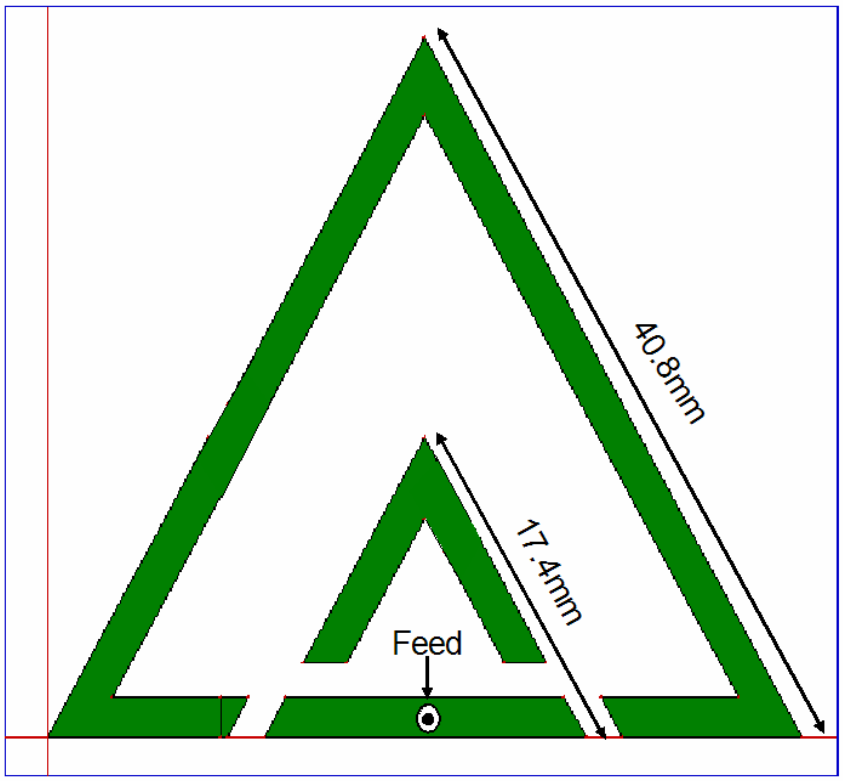

Figure 19 : The reconfigurable center-fed equilateral triangular loop antenna with all the switches open

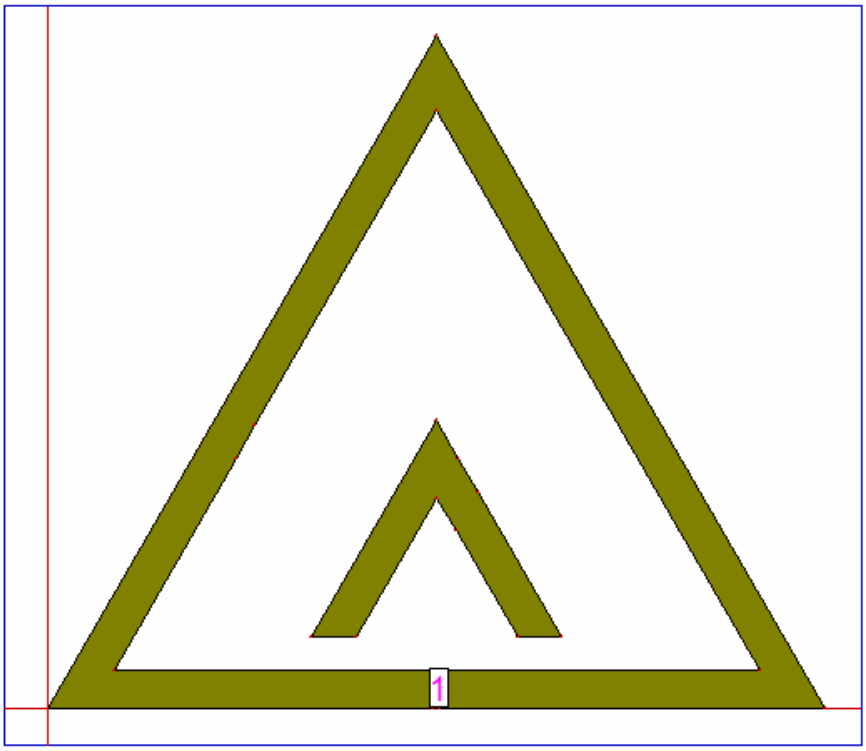

Figure 20 : The reconfigurable center-fed equilateral triangular loop antenna with the closed switches for the 2.45GHz operation.

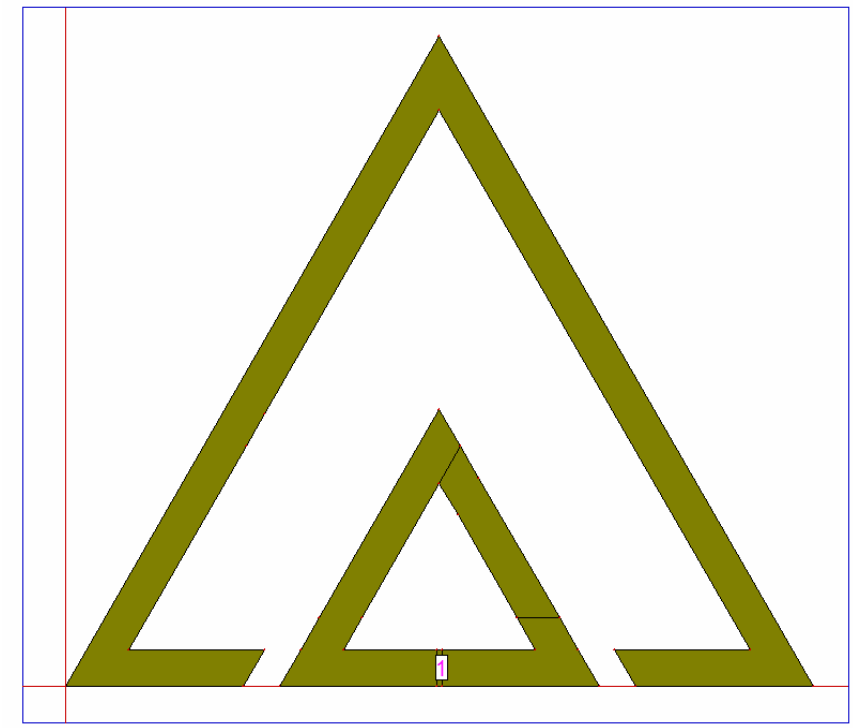

Figure 21: The reconfigurable center-fed equilateral triangular loop antenna with the closed switches for the 5.78GHz operation.

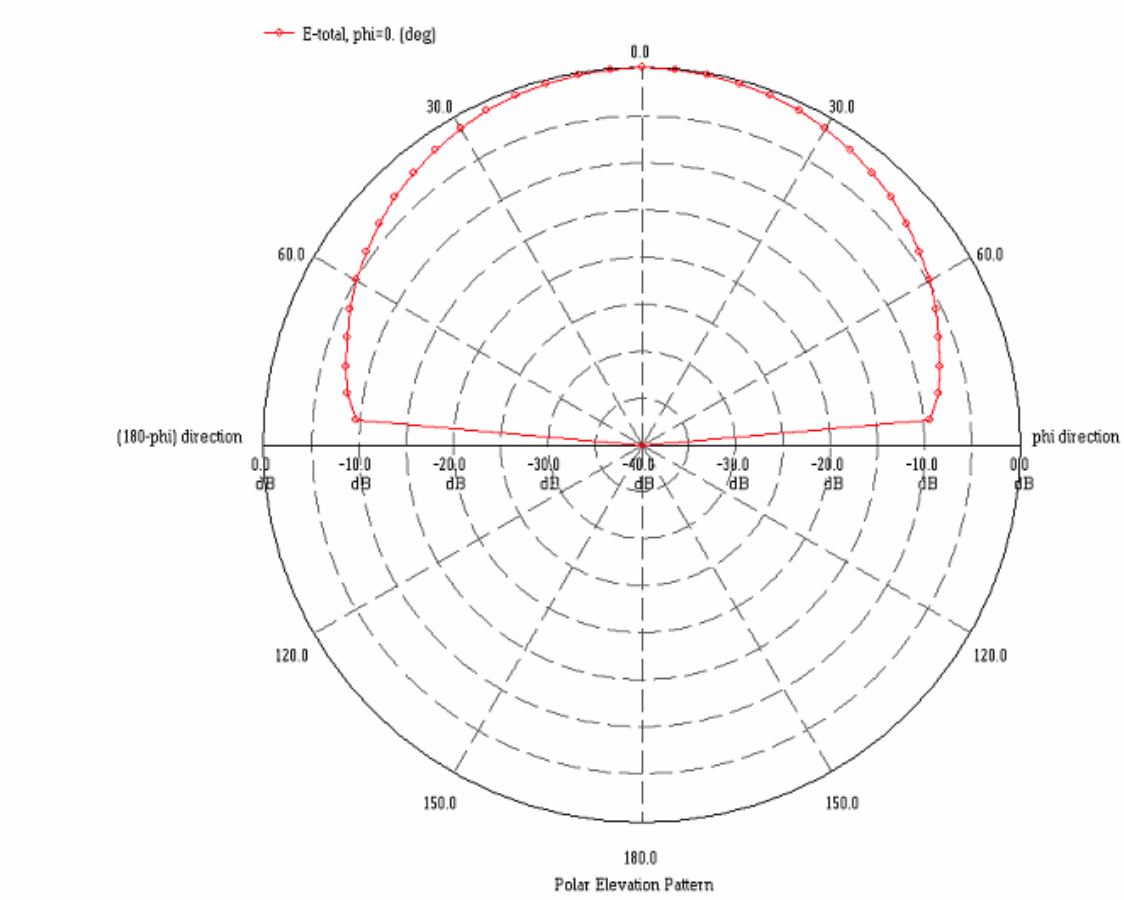

Figure 22: Radiation pattern in the elevation Plane (φ=0º) for the reconfigurable center-fed equilateral triangular loop antenna at 2.45GHz.

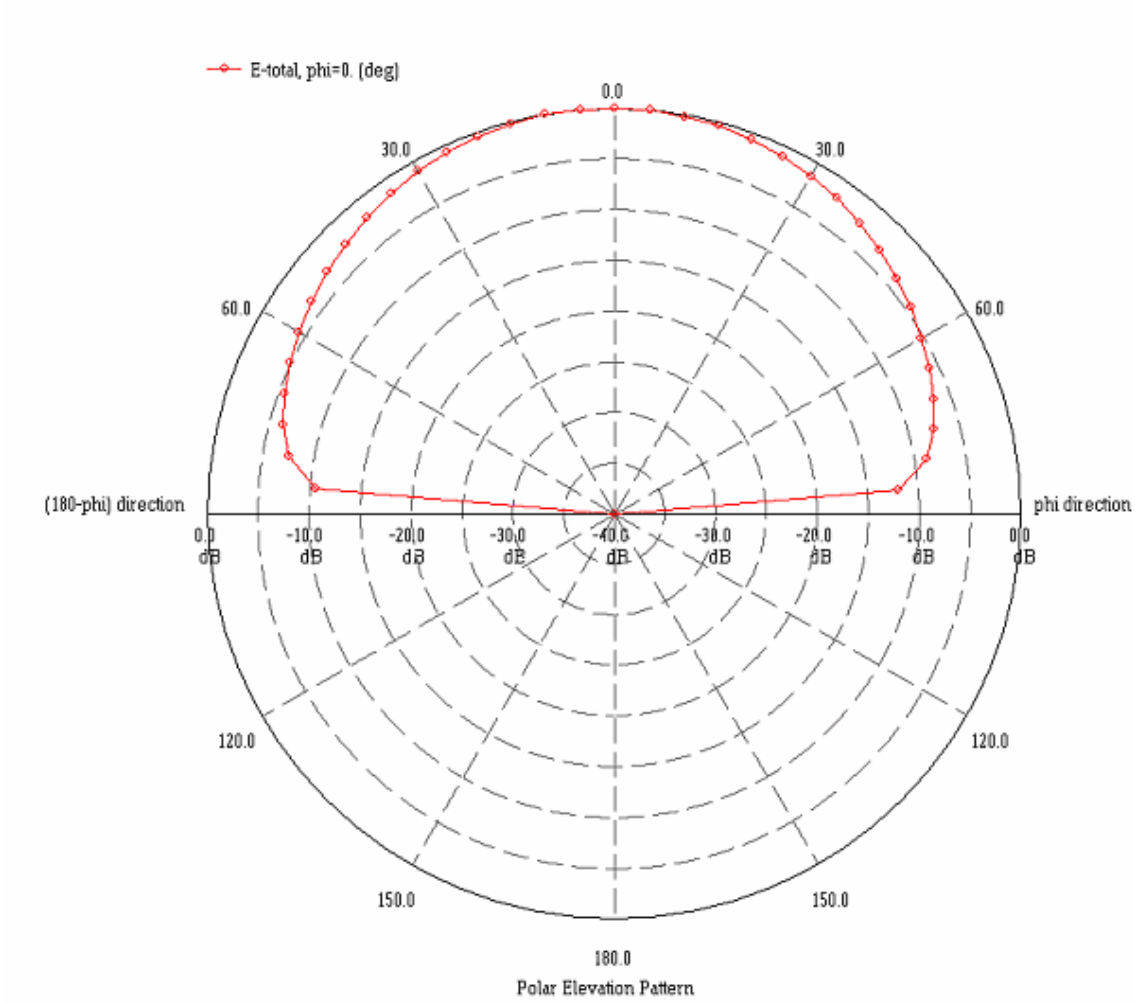

Figure 23: Radiation pattern in the elevation plane (φ=0º) for the reconfigurable center-fed equilateral triangular loop antenna at 5.78GHz.

Reconfigurable Rectangular-spiral Antenna

Both types of reconfigurable equilateral triangular loop antennas presented above have very good performance and are much smaller in dimensions compared to the reconfigurable Yagi antenna. In our search to find an even more compact reconfigurable antenna, we designed the reconfigurable rectangular spiral antenna. It is about 50% smaller than the reconfigurable equilateral triangular loop antenna at each of the frequencies, 2.45GHz and 5.78GHz. As shown in Figure 24, the largest dimensions are 20mm x 20mm, and in addition it requires only one switch, which makes it less expensive compared to the other antennas. It was found that the spiral length and the placement of the switch were critical in getting wide beamwidth as desired for both the design frequencies. The optimum beamwidth was obtained at the spiral length of 120mm for 2.4GHz and 64mm for 5.78GHz, which is around one wavelength at each of the operating frequencies. At 2.45 GHz it has a 3dB beamwidth of 85.6^0 and directivity of 6.5 dB. As for the 5.78GHz frequency the 3dB beamwidth is 82.5^0 and the directivity is 7.16 dB. Figure 25 and Figure 26 show the reconfigurable rectangular spiral antenna for the 2.45GHz and the 5.78GHz operation respectively. Simulated radiation patterns in the elevation plane ($\varphi=0^o$) at the two frequencies are shown in Figure 27 and Figure 28 respectively.

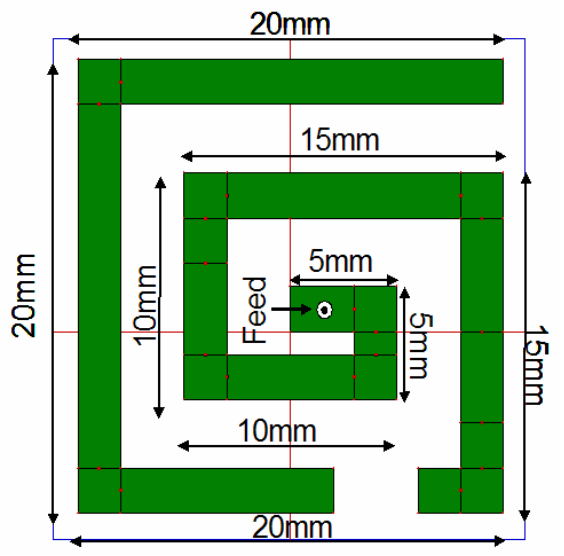

Figure 24: The reconfigurable rectangular-spiral antenna with the switch open

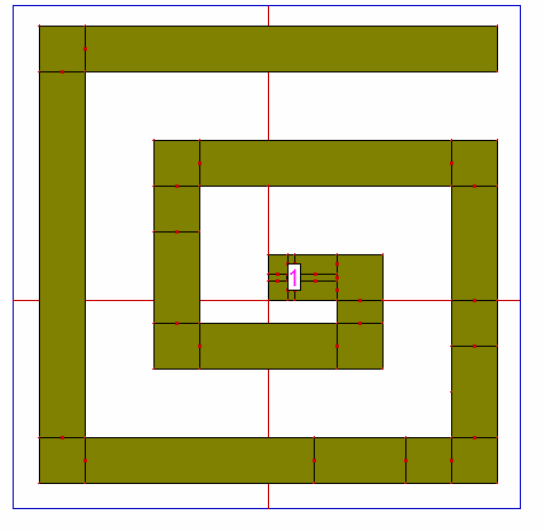

Figure 25: The reconfigurable rectangular-spiral antenna for the 2.45GHz operation

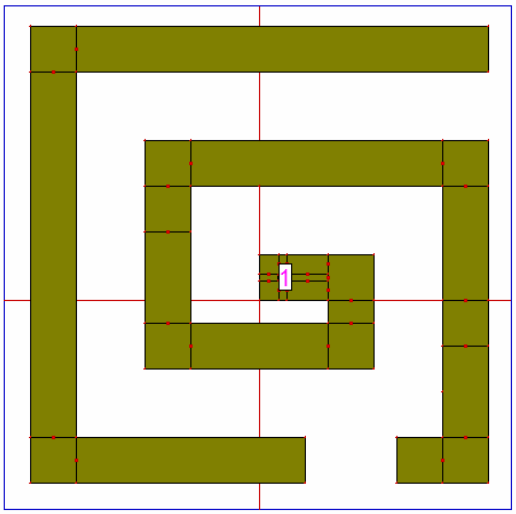

Figure 26: The reconfigurable rectangular-spiral antenna for the 5.78GHz operation

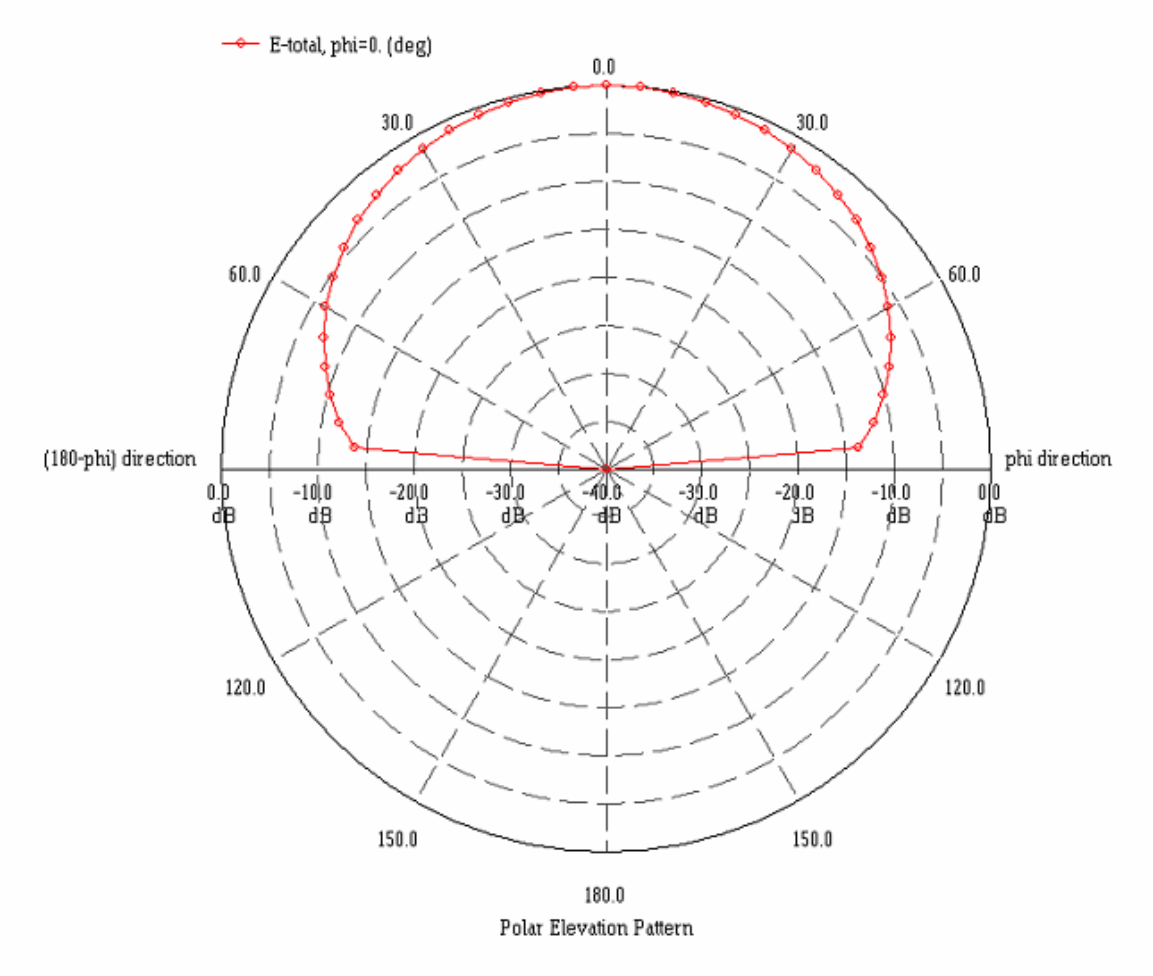

Figure 27: Simulated radiation pattern in the elevation plane (φ=0º) for the reconfigurable rectangular-spiral antenna at 2.45GHz

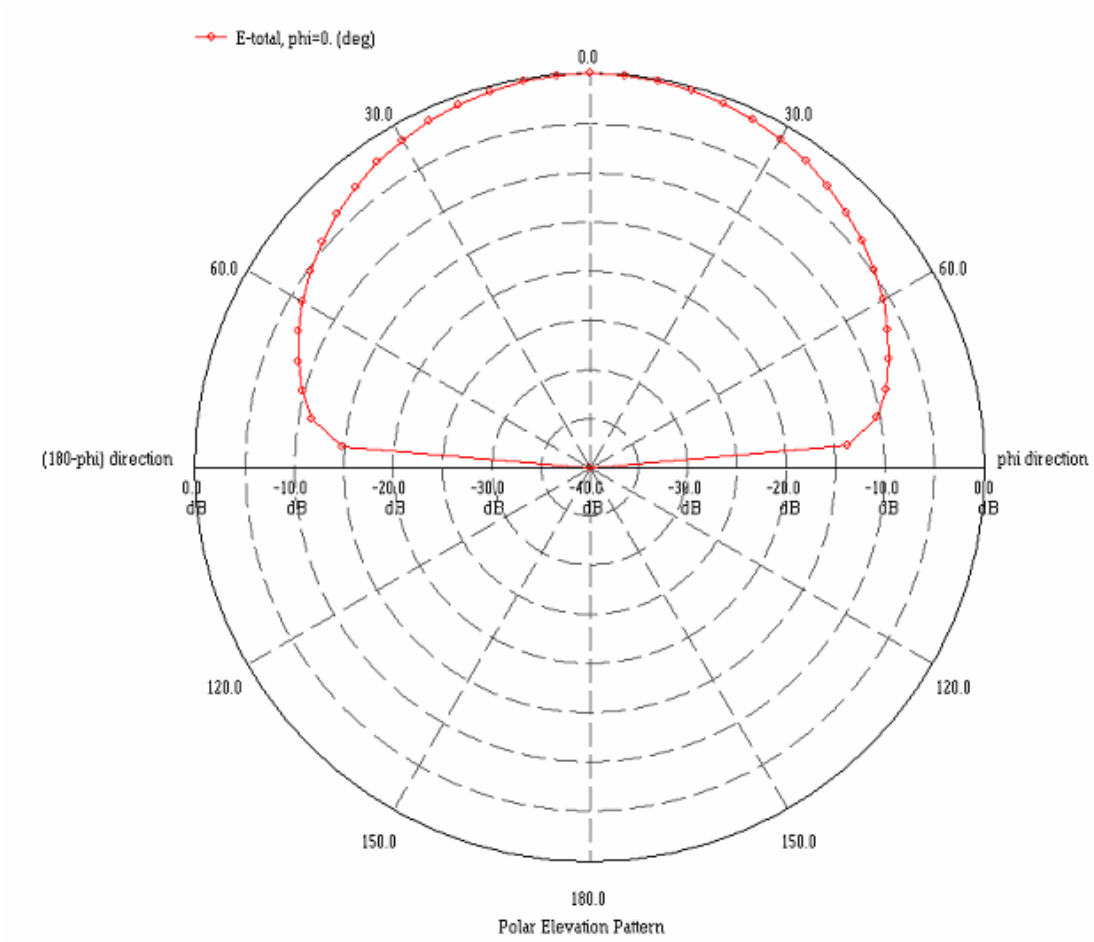

Figure 28: Simulated radiation pattern in the elevation plane (φ=0º) for the reconfigurable rectangular-spiral antenna at 5.78GHz

Conclusion

In this chapter reconfigurable antennas and their advantages were discussed. Four novel reconfigurable elements were presented. The reconfigurable Yagi measures (60mm X 175.01mm) and uses 12 switches to enable the reconfiguration between the 2.45GHz frequency operation and the 5.78GHz frequency operation. At 2.45 GHz the antenna has a 3db beamwidth of 57.6^0 and a directivity of 8.62 dB. At 5.78 GHz the antenna has a 3db beamwidth of 37.4^0 and a directivity of 11.49 dB.

Two types of the reconfigurable triangular loop antenna were designed, the corner-fed and the center-fed. Both of them are more suitable for wireless LAN applications than the Yagi antenna. With a maximum dimension of 40.8mm, both of them are much more compact, they also have broader beamwidth and are less expensive because they require only 4 switches for reconfiguration. At 2.4GHz the corner-fed antenna has a 3dB beamwidth of 78.6^0 and a directivity of 8.07 dB. At 5.78GHz the 3dB beamwidth is 94^0 and the directivity is 7.175 dB. The center-fed exhibits slightly better performance than the corner-fed. It has a 3dB beamwidth of 89.25^0 and directivity of 7.1 dB at the 2.45 GHz operating frequency. For the 5.78GHz configuration it has 94.7º beamwidth and the directivity is 6.8 dB.

An even more compact antenna was designed which is the reconfigurable rectangular spiral. Its maximum dimension is only 20mm. It has only one switch which makes it cheaper to fabricate.

The reconfigurable rectangular spiral has a 3dB beamwidth of 85.6^0 and directivity of 6.5 dB at 2.45GHz. As for the 5.78GHz frequency the 3dB beamwidth is 82.5^0 and the directivity is 7.16 dB.

CHAPTER 4: ADAPTIVE AND RECONFIGURABLE ANTENNAS

Introduction

An adaptive system consisting of an antenna array and an adaptive processor can perform filtering both in the space and the frequency domains, thus reducing the sensitivity of the signal-receiving system to interfering directional noise source.

Through the use of MEMS switches, PIN switches, or other switching mechanisms, a reconfigurable antenna can be structurally reconfigured to maintain its elements near their resonant dimensions for several frequency bands. This increases the bandwidth of the antenna dramatically, which allows one antenna to be used for several applications such as wireless, radar etc. Reconfigurable antennas can save weight, space and money.

In this chapter we introduce a novel type of antenna that combines adaptivity and reconfigurability. An adaptive antenna that can null interference and steer its main beam towards a desired signal and at the same time be reconfigurable to maintain functionality at several frequency bands has the potential to revolutionize wireless communication in the future. Combining reconfigurability with adaptivity is still not reported in the literature. Through

several examples it is shown that this new type of antennas, namely adaptive and reconfigurable arrays, is indeed feasible and show very good results.

Adaptive and Reconfigurable Antenna

We start by a simple example of an adaptive and reconfigurable antenna to demonstrate feasibility. The array shown in Figure 29 is a two element reconfigurable half wavelength antenna operating at frequency f_1 and $f_2 = 2\ f_1$. With the switches open the dipoles operate at f_2, and when closed the dipoles operate at f_1. The distance between the elements is fixed at $d = \lambda_2/2 = \lambda_1/4$.

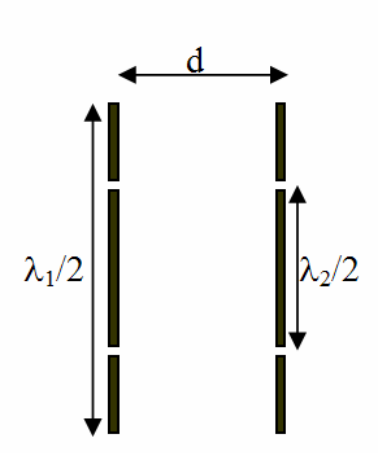

Figure 29: Two-element reconfigurable dipole antenna array

The adaptive configuration is shown in Figure 30. It is the same configuration as that used in the example in Chapter 2.

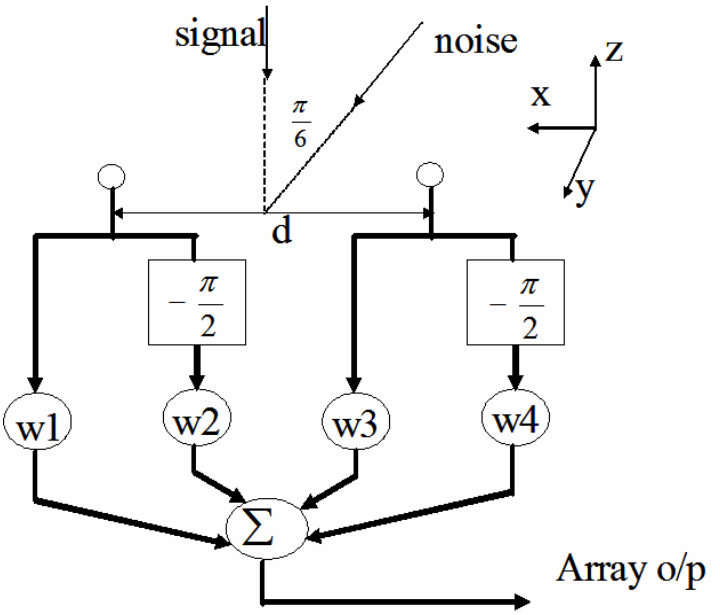

Figure 30: The adaptive configuration to eliminate the noise incident on the array at 30º.

We want to have the antenna adaptively eliminate a noise signal incident on the array at 30° at both the operating frequencies. Before adaptation the weights are w1 = w3 = 1 and w2 = w4 = 0. At the higher frequency, ignoring the mutual coupling effects the adaptive weights obtained are: w1 = w2 = w3 = 0.495, w4 = -0.496 whereas at the lower frequency the weights are: w1 = 0.51, w2 = 1.18, w3 = 0.48 and w4 = -1.184.

Figure 31 and Figure 32 show that the adaptive algorithm seems to successfully eliminate the noise incident at 30° on the reconfigurable array.

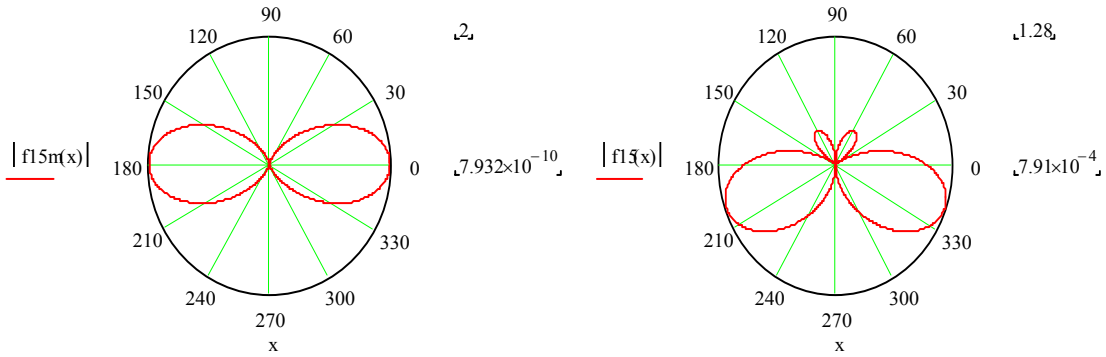

Figure 31 : The directivity pattern for the reconfigurable adaptive antenna at the higher frequency, (i.e. with switches left open) , when mutual coupling is ignored. Figure 31a shows the non-adaptive directivity pattern, Figure 31b shows the adaptive antenna successfully nulling the noise incident at 30 degrees

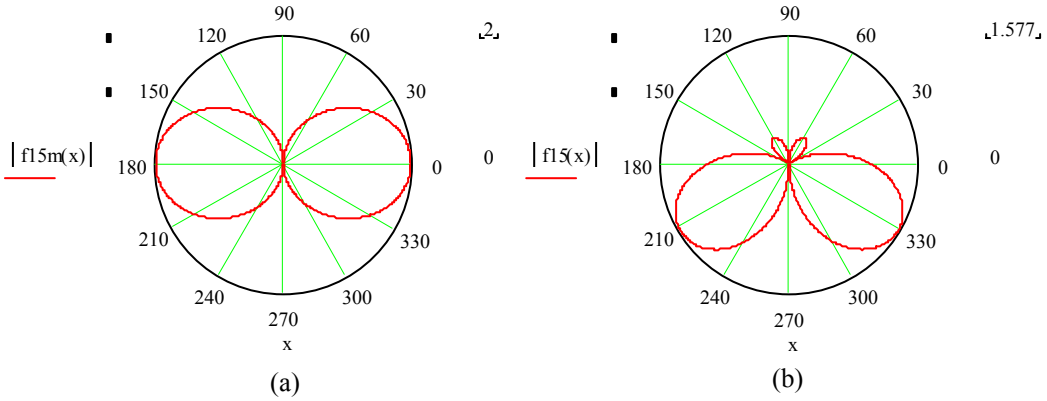

Figure 32: The directivity pattern for the reconfigurable adaptive antenna at the lower frequency,(i.e. with switches closed), when mutual coupling is ignored. Figure 32a shows the (non-adaptive) directivity pattern, Figure 32b shows the adaptive antenna successfully nulling the noise incident at 30 degrees

When the mutual coupling effects are included, the adaptive algorithm deteriorates as shown in Figure 33. We note that the performance is worse for the lower frequency because the distance d in terms of wavelengths becomes smaller for the lower frequency, thus the array has more mutual coupling due to the reduced interelement spacing. This shows again how important it is to include and compensate the effect of mutual coupling in the adaptive algorithm especially when dealing with an adaptive and reconfigurable array as the interelement spacing become smaller in terms of wavelength for the lower frequencies of the array.

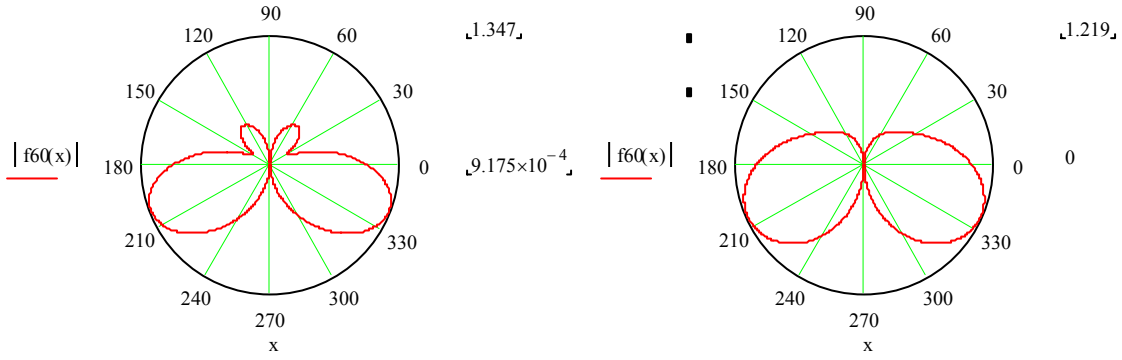

(a) (b)

Figure 33: The directivity pattern for the reconfigurable adaptive antenna at the higher frequency, Figure 33a, and at the lower frequency, Figure 33b, with mutual coupling effect.

As the feasibility of the novel idea of combining adaptivity with reconfigurability was demonstrated above, the following section will demonstrate using the reconfigurable elements presented in Chapter 3 in an array and making this array adaptive. By doing this we present the first antenna array of its kind. Note that because the reconfigurable elements are in an adaptive array, which can direct its main beam towards the desired signal while nulling interferences incident on the array from other directions, the radiation pattern of the array is not required to have broad beam-width or near omni- directional coverage to be used in WLAN communications.

Adaptive and Reconfigurable Equilateral Triangular Ring Array

In this section the reconfigurable equilateral triangular loop introduced in chapter 3, will be used in an adaptive array. The LMS adaptive algorithm is used. In the LMS algorithm the number of interferences, "I", an array of with number of elements "N" can eliminate is given by Equation (3.2).

$$I=N-1 \tag{3.2}$$

In the following examples it is desired to null noises incident on the array from two different directions, therefore three elements are used.

The 3-element reconfigurable equilateral triangular loop array is shown in Figure 33 (a) and Figure 33(b) for the 2.4GHz and the 5.78GHz operation respectively. The distance between the elements is d=61.2 mm which corresponds to a spacing of 0.5λ at 2.45GHz and 1.2λ at 5.78GHz. The adaptive configuration used to null the noises incident on the array at +/- 30^0 is shown in Figure 34. Before applying the adaptive algorithm, the weights attached to the elements are w1=w3=w5=1 and w2=w4=w6=0. Using the LMS algorithm we want to solve for the weights values required to eliminate the noise incident on this array while maintaining the desired signal incident on the array at 0^0.

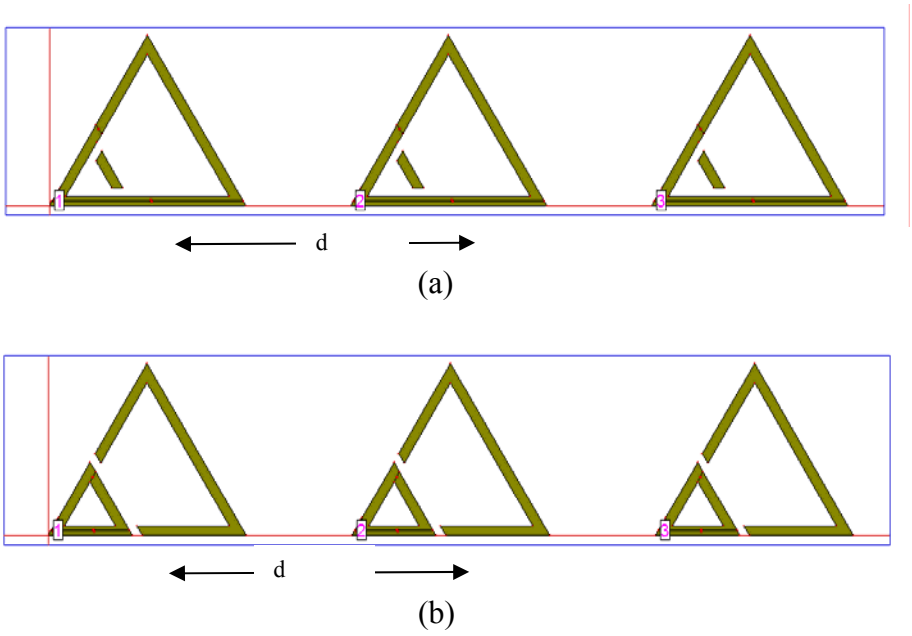

Figure 33: Array of reconfigurable equilateral triangular loop with d =61.2mm : (a) at the 2.45GHz frequency , (b) at the 5.78GHz frequency

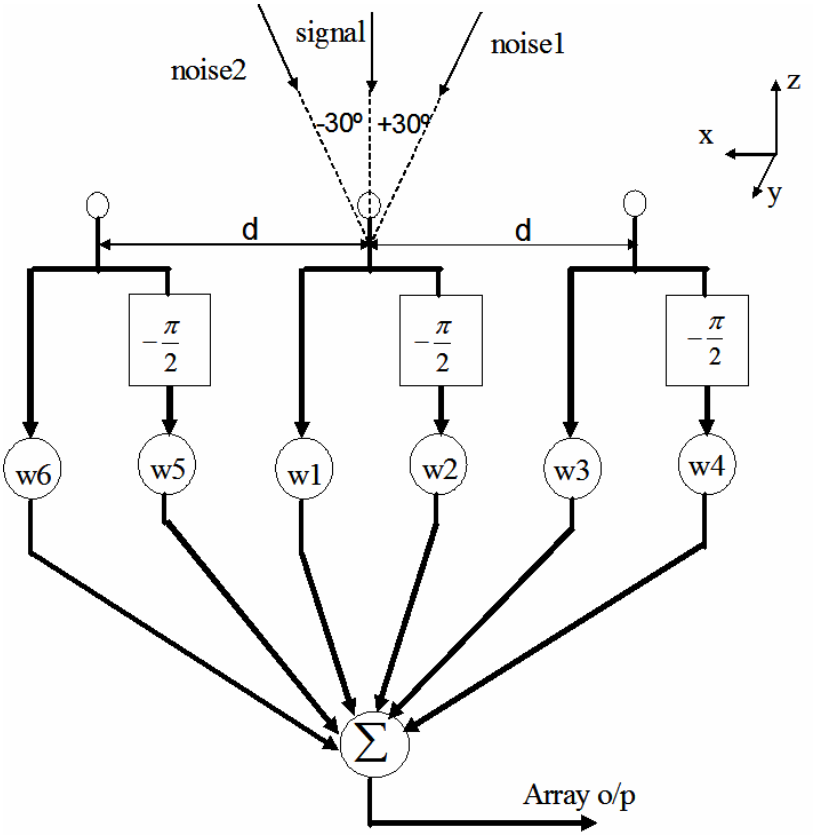

Figure 34 : Adaptive configuration to eliminate noises incident on the array at +/- 30º

In this example the LMS algorithm solution for the weights for f=2.45GHz, d=λ/2: w1 = w2 = w4 = w6 =0, w3 = w5 = 0.5. Figure 35 shows the array radiation pattern at 2.45GHz before implementing the adaptive algorithm. Figure 36 shows deep nulls at +/- 30^0 in the radiation pattern after the adaptive algorithm is implemented. This means the noises were successfully eliminated.

For f=5.78GHz, d=1.2λ, the LMS solution for the weights are: w2=w6=w4=0, w3=w5=0.2764 and w1=0.447. Figure 37 shows the non-adaptive array radiation pattern at 5.78GHz, while Figure 38 shows the radiation pattern after noise elimination using the adaptive algorithm. As can be seen, deep nulls were again successfully placed at +/-30º, thus eliminating the incident noises as desired, while maintaining the desired signal incident at 0º.

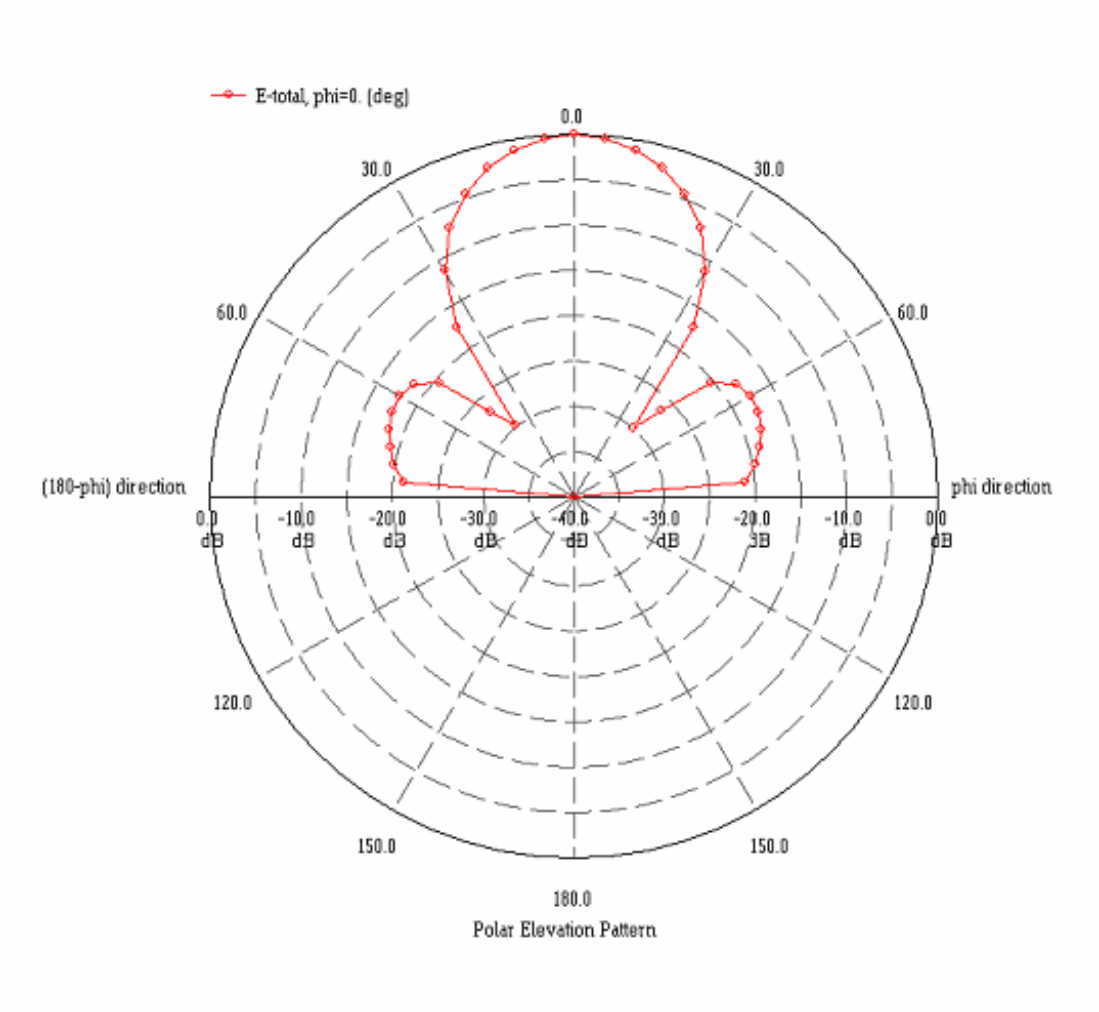

Figure 35: Non-adaptive radiation pattern of the 3-element reconfigurable equilateral triangular loop array at 2.4GHz.

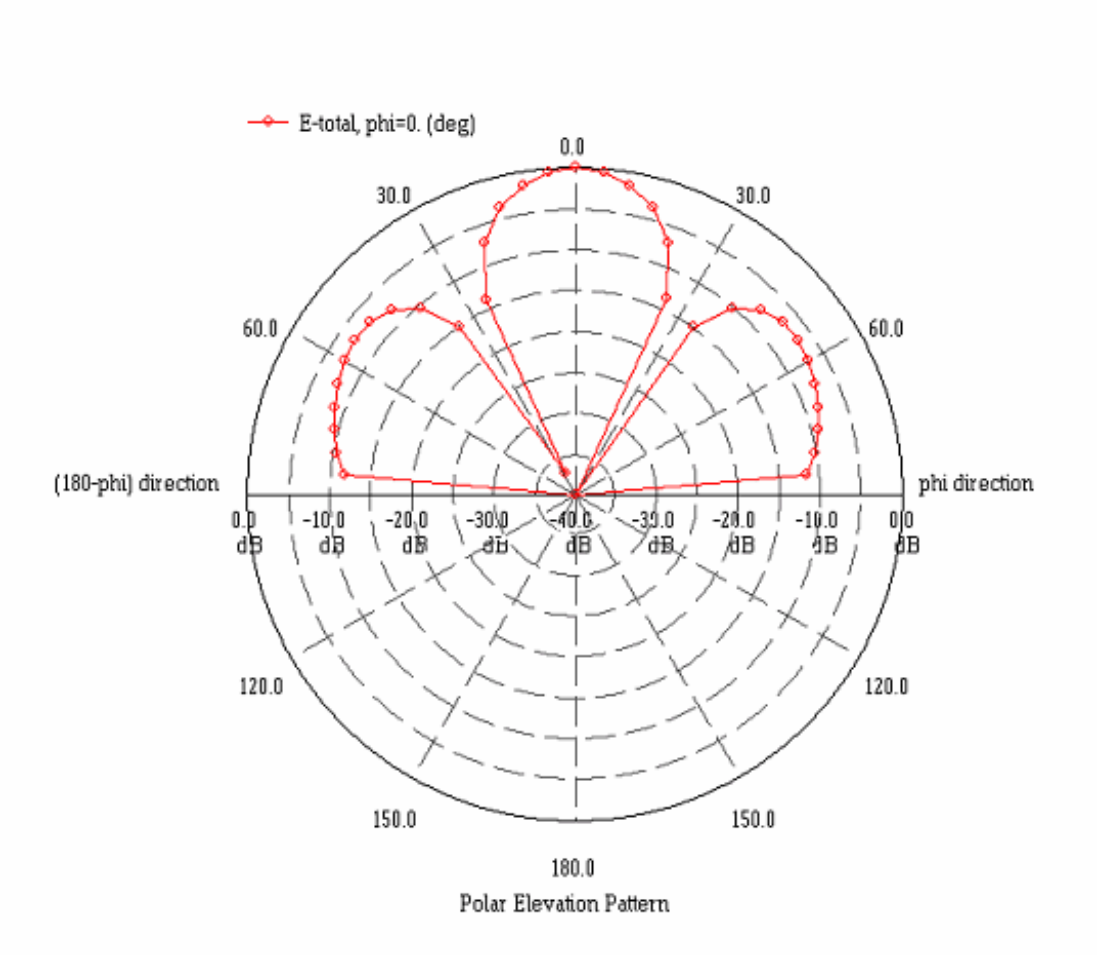

Figure 36: Adaptive radiation pattern of the 3-element equilateral triangular loop array at 2.4GHz after eliminating the noise incident at +/- 30 degrees while maintaining the desired signal at zero degrees

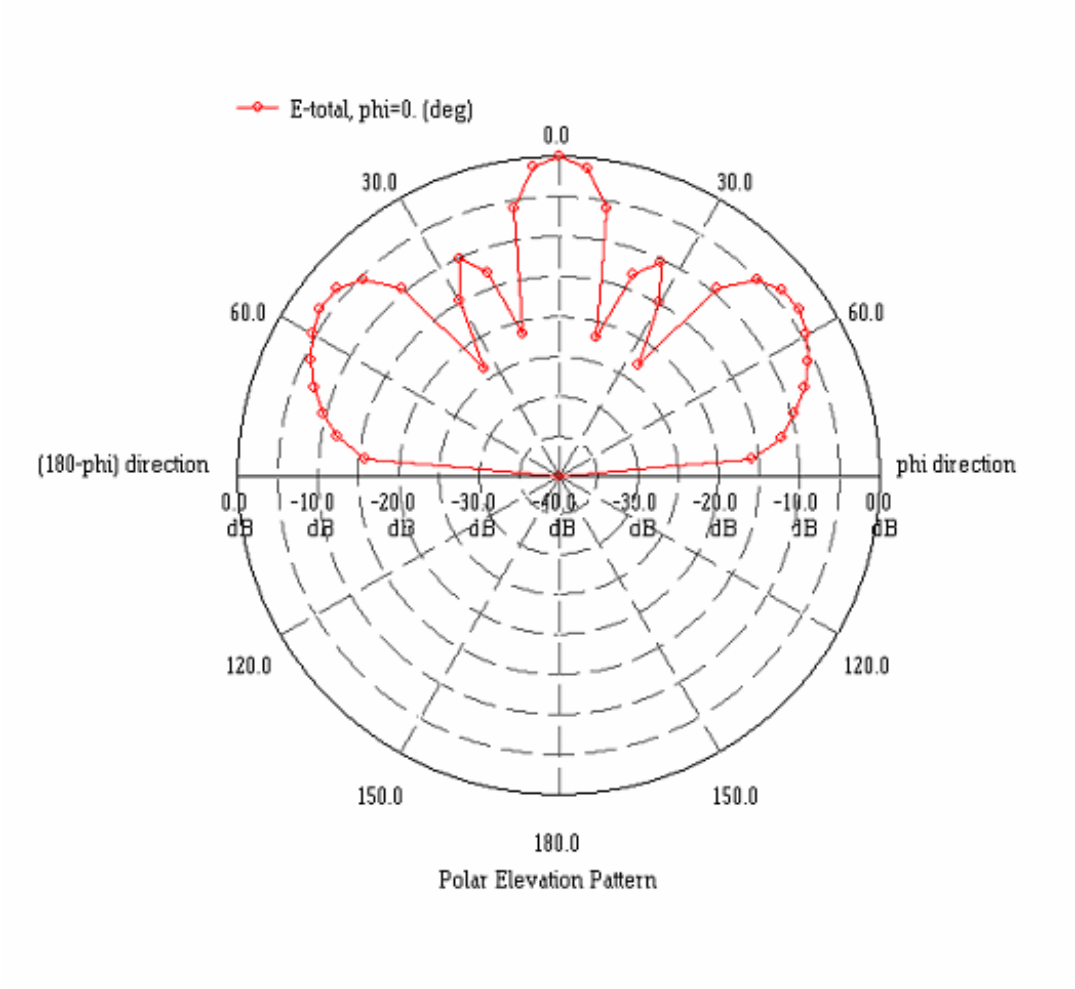

Figure 37: Non-adaptive radiation pattern of the 3-element reconfigurable equilateral triangular loop array at 5.78GHz before noise elimination

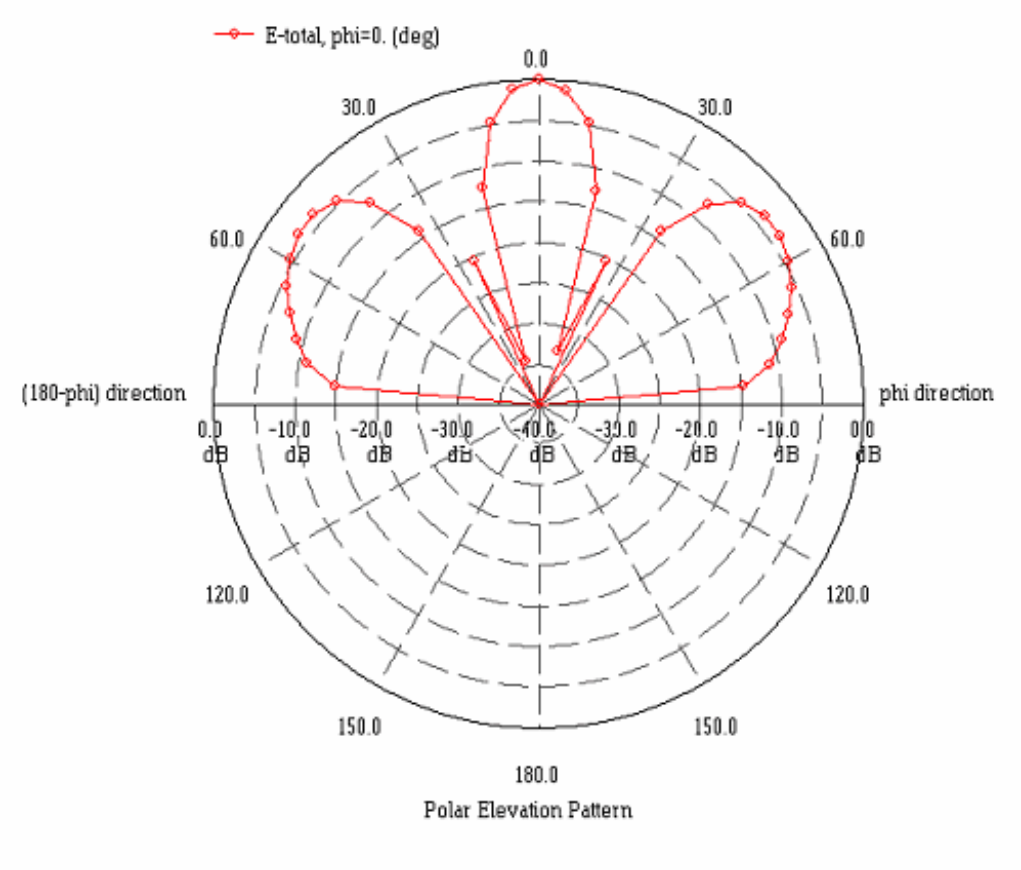

Figure 38: Adaptive radiation pattern of the 3-element reconfigurable equilateral triangular loop array after eliminating the noise incident at +/- 30 degrees, while maintaining the desired signal at zero degrees

Adaptive and Reconfigurable Rectangular-spiral Array Antenna

As another example of combining adaptivity with reconfigurability, the reconfigurable rectangular-spiral antenna element presented in Chapter 3 is used in an adaptive array. Utilizing the advantage of the small dimension of the reconfigurable rectangular-spiral antenna, the elements can be placed closer together in the array. As shown in Figure 39 the 3-element array have the distance d=25.95mm between the elements. This is equivalent to d=0.21 λ for the 2.45 GHz array configuration and d=0.5λ for f=5.78GHz.

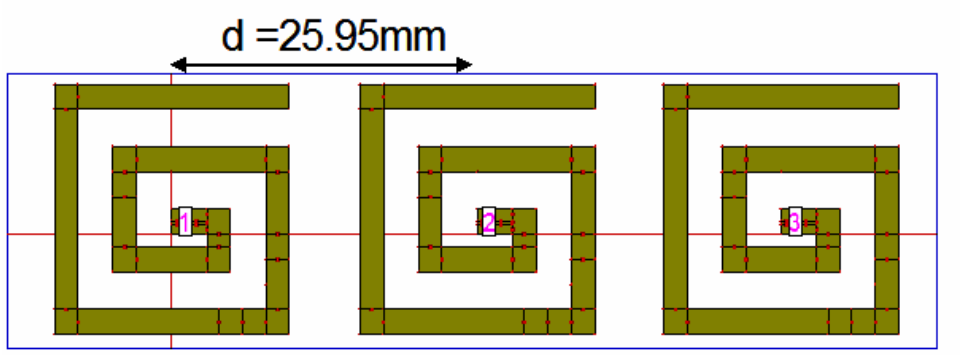

(a)

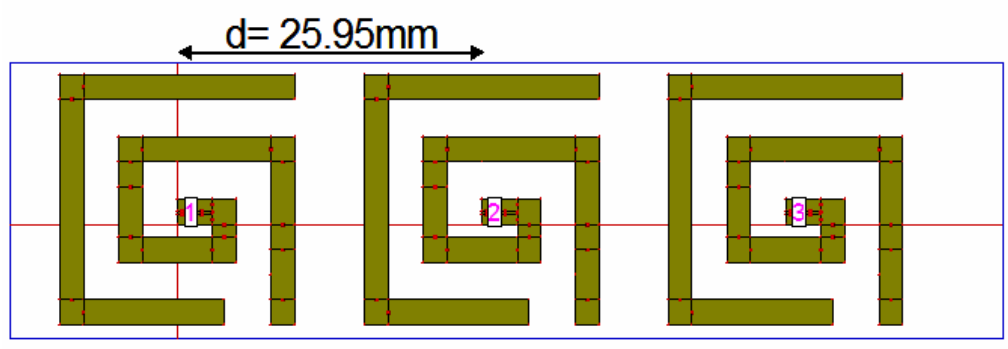

(b)

Figure 39: 3-element reconfigurable rectangular-spiral array configuration: (a) at f=2.45GHz, (b) at f=5.78GHz

The adaptive configuration for this antenna is shown in Figure 40. The noise to be eliminated is incident on the array at +30º/+60º. The desired signal is again incident at 0º.

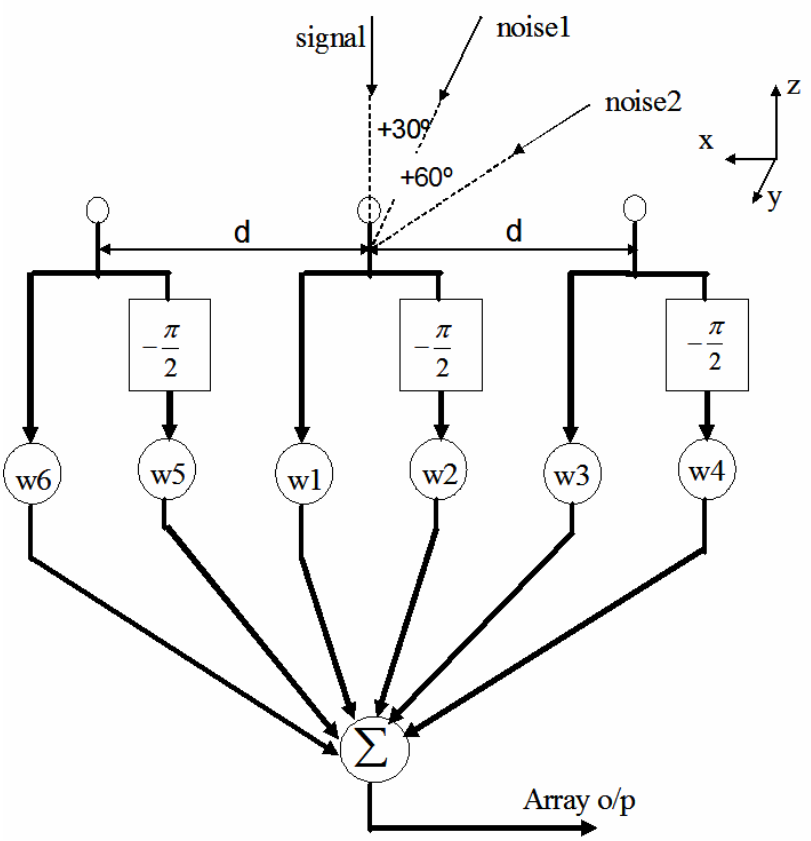

Figure 40: Adaptive configuration used to eliminate noises incident at +30º/+60º

For the array configuration at 2.45GHz the solution for the weights using the LMS algorithms is: w1 =3.03, w2 =0, w3 =-1.015, w4 =-1.18, w5 = w3 and w6 = -w4. Figure 41 shows the radiation pattern of the array at 2.45GHz before noise elimination and Figure 42 after noise has been eliminated adaptively. As can be seen the noise incident at +30/+60 are successfully eliminated. Figure 42 show also that value of the desired signal at 0º is reduced in magnitude after the adaptive process. However the array output due to the incident signal at 0º is still much higher

than the output due to the noises at +30º/+60º. The power signal to noise ratio in this case is more than 46 dB. Thus here again the array have successfully eliminated the noise while maintaining the reception of the desired signal.

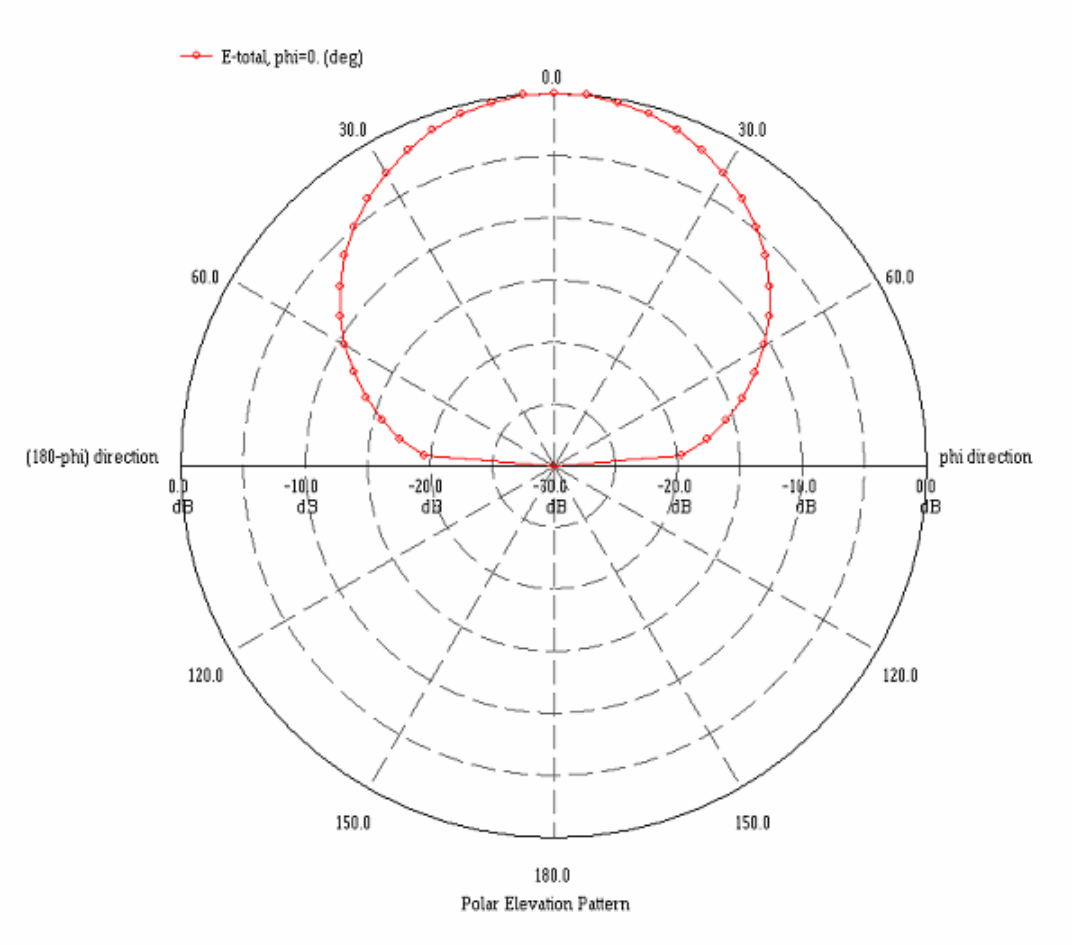

Figure 41: Radiation pattern of the reconfigurable rectangular spiral array at 2.45GHz before noise elimination.

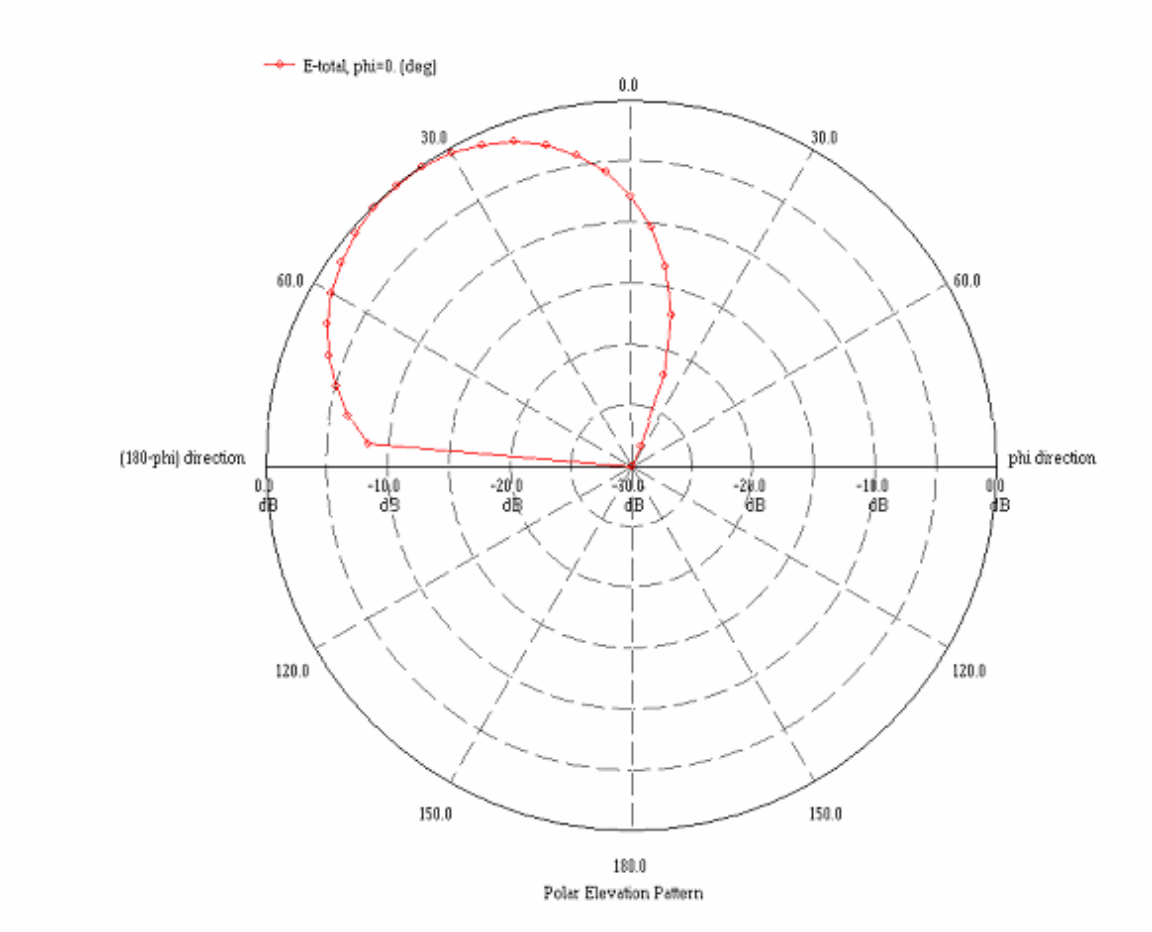

Figure 42: Radiation pattern of the reconfigurable rectangular spiral array at 2.45GHz after noise elimination.

For the 5.78GHz array, the LMS algorithm solution for the weights is: w1=0.607, w2=0, w3=1.97, w4=-0.303, w5=1.97, w6=0.303. Figure 43 shows the radiation pattern of the 3-elemnet reconfigurable rectangular-spiral array at 5.78GHz before adaptation, while Figure 44 shows it after successful elimination of noise at +30º/+60º.

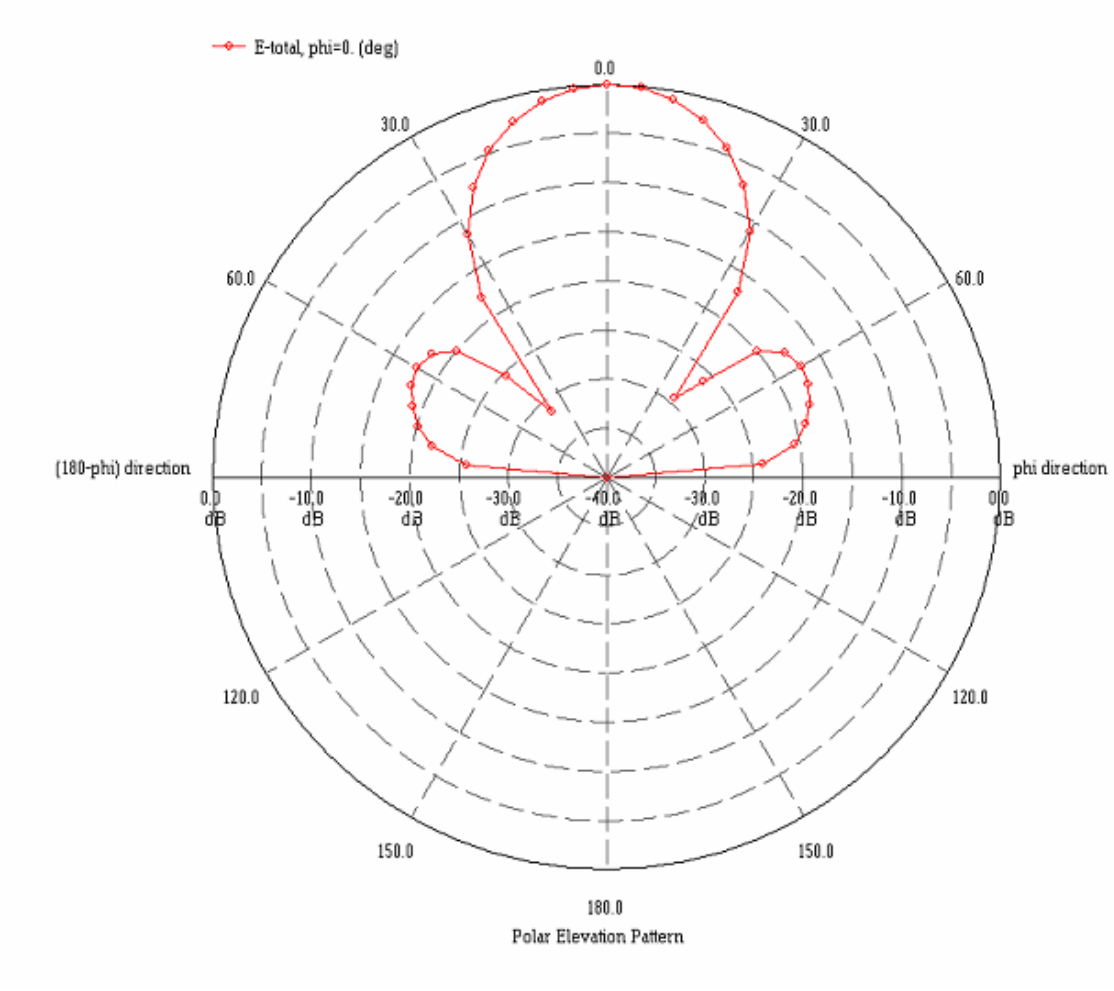

Figure 43: Radiation pattern of the adaptive and reconfigurable rectangular-spiral antenna array at 5.78GHz before noise elimination.

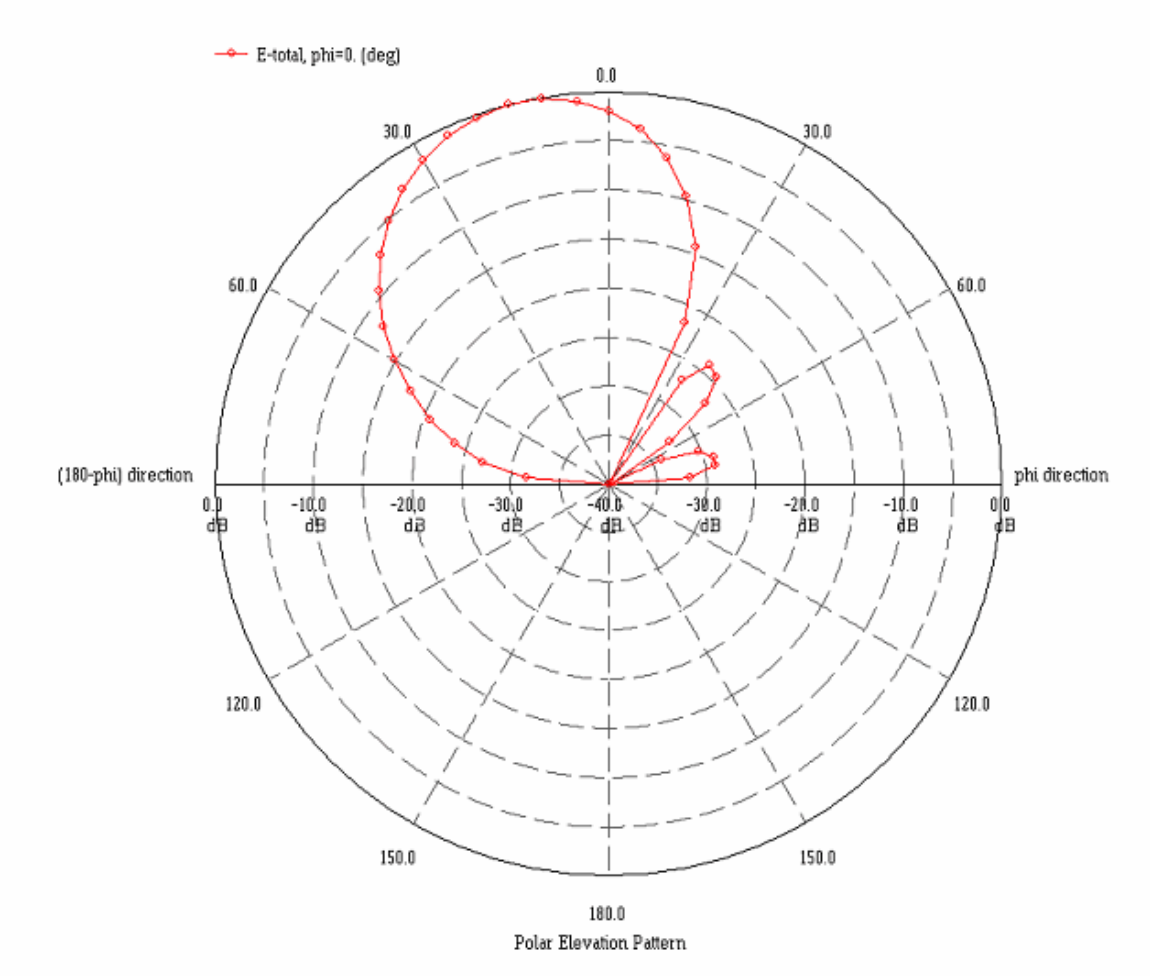

Figure 44: Radiation pattern of the adaptive and reconfigurable rectangular-spiral antenna array at 5.78GHz after noise elimination.

As a final example to demonstrate the combination of adaptivity and reconfigurability , the same reconfigurable rectangular spiral-array shown in Figure 39 (a) and (b) for the frequencies 2.45 and 5.78GHz respectively is used in an adaptive configuration to eliminate noises incident on the array from two different directions +30º/-60º as shown in Figure 45.

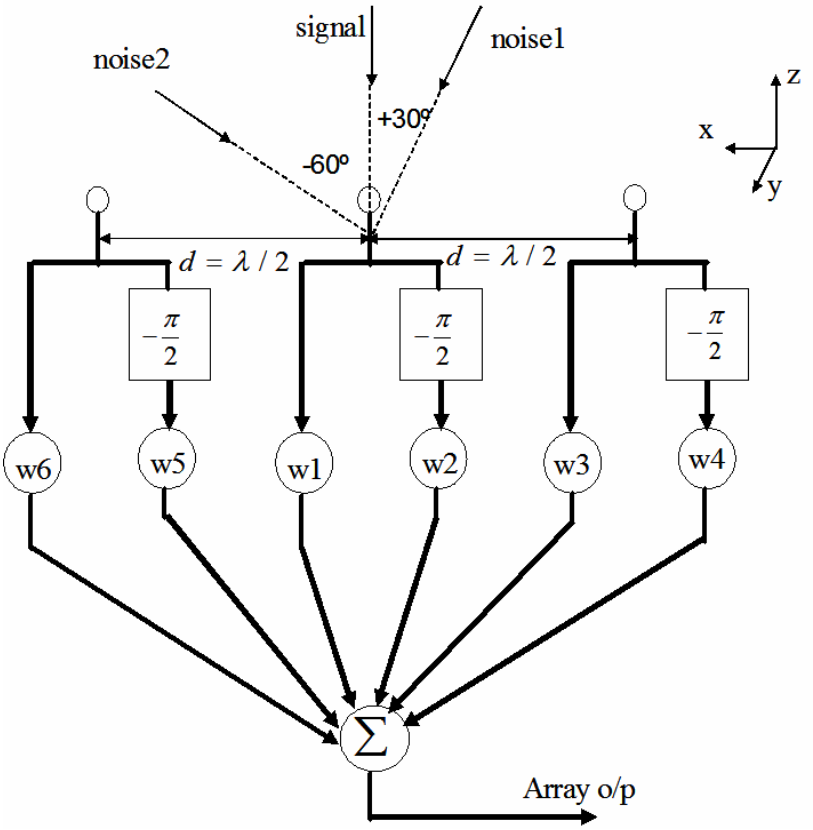

Figure 45 Adaptive configuration used to eliminate noises at +30º/-60º

The LMS algorithm solution for the weights at 2.45GHz is: w1 = -1.723, w2 = 0, w3 = 1.362, w4 = -0.339, w5 = w3, w6 = -w4. The noise from +30º/-60º is successfully eliminated as displayed in Figure 46.

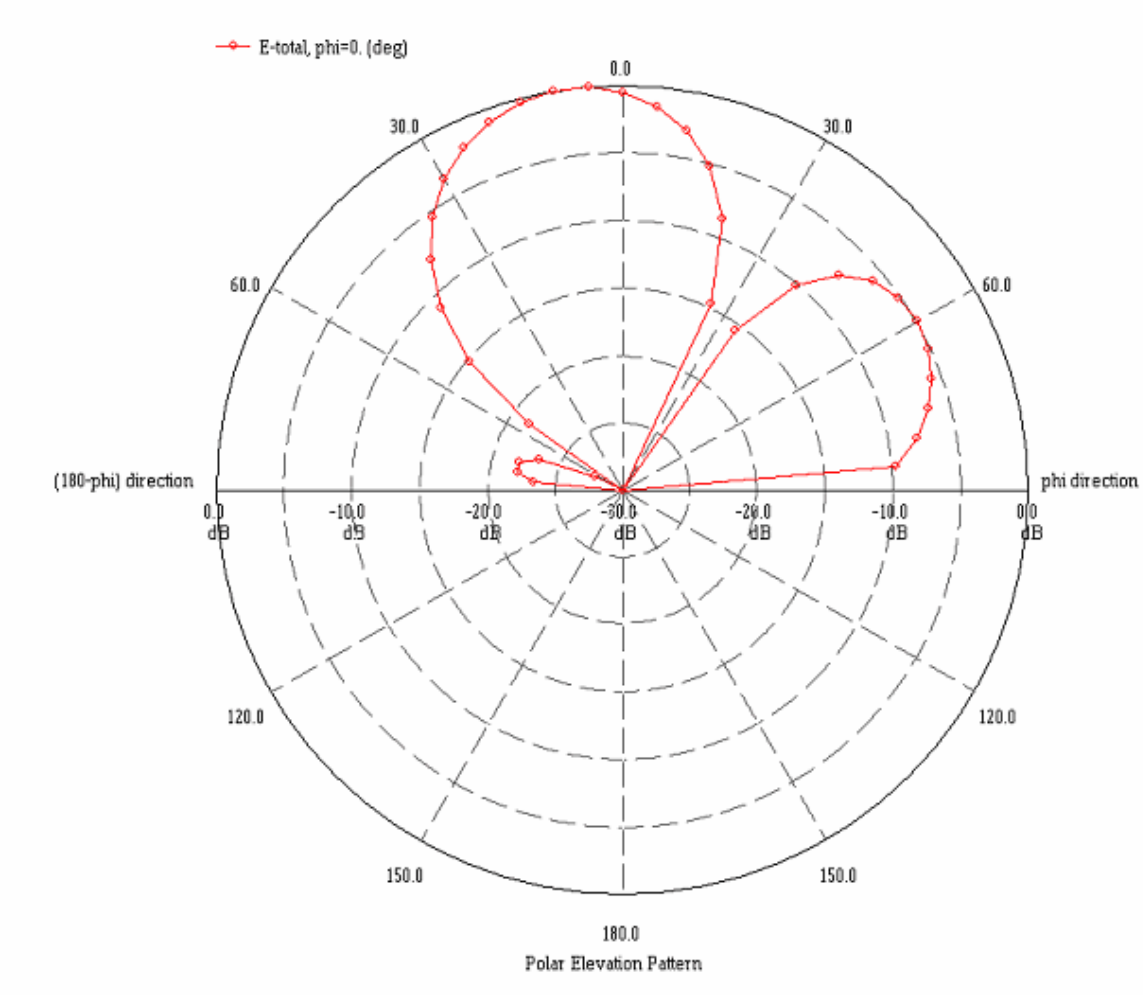

Figure 46: Radiation pattern of the adaptive and reconfigurable rectangular-spiral antenna array at 2.45GHz after elimination of the noise at +30º/-60º

The weights required to eliminate the noises at +30º/-60º for the adaptive and reconfigurable rectangular-spiral antenna array at 5.78GHz were found using the LMS algorithm to be: w1=0.393, w2=0, w3=0.303, w4=-0.197, w5=0.303 and w6=0.197. Figure 47 shows that the noises incident on the array at +30º/-60º were indeed eliminated as desired.

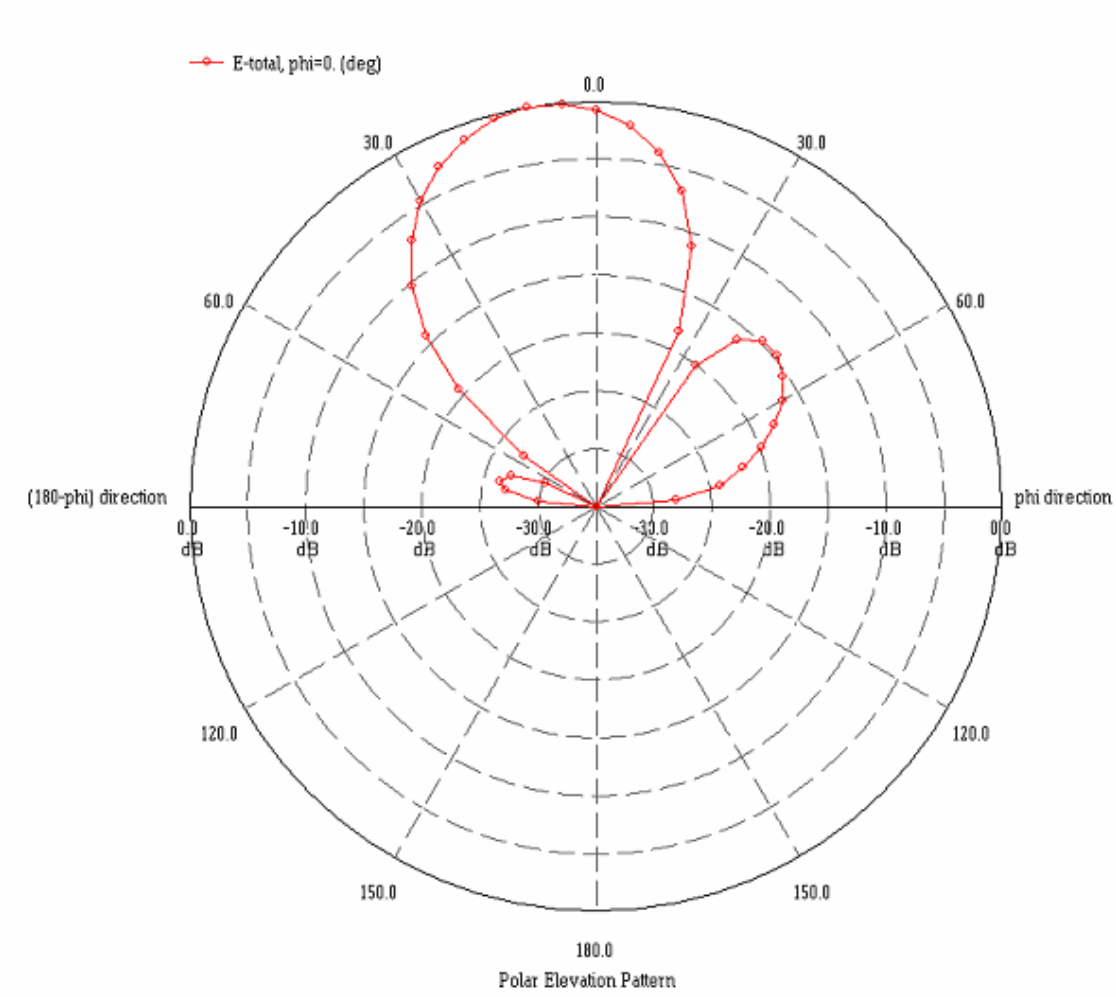

Figure 47: Radiation pattern of the adaptive and reconfigurable rectangular-spiral antenna array at 5.78GHz after noise elimination+30º/-60º

Conclusion

In this chapter a novel type of antenna array was presented, combining reconfigurable elements and an adaptive processor. This has not been reported before in the literature. Several example demonstrated the feasibility and effectiveness of this type of antenna. In this chapter the basic LMS adaptive algorithm was used.

CHAPTER 5: CONCLUSION

Adaptive array antennas with their ability to automatically respond to an unknown interference environment by steering nulls and reducing sidelobe levels in the direction of the interference, while maintaining some desired signal beam characteristics have been studied. The effect of mutual coupling on adaptive array was analyzed using the method of moments. It was shown that the mutual coupling effect on adaptive arrays is detrimental and thus can't be ignored even for large interelement spacing. Ignoring the mutual coupling causes the adaptive algorithm to be inaccurate. A method to compensate for the mutual coupling effect was tested and found to be useful. This method is based on recognizing that the MOM voltage vector is free from mutual coupling. Solving for MOM voltage vector using the received voltage and the MOM admittance matrix enables the adaptive processor to solve for the adaptive weights correctly and such successfully nulling the incident noise.

The reconfigurable antenna is a promising and exciting new type of antenna, where through the use of appropriate switches, the antenna can be structurally reconfigured to maintain the elements near their resonant dimensions for several frequency bands. This increases the bandwidth of the antenna dramatically, which enables the use of one antenna for several applications, wireless, radar etc. This is particularly important for satellite application where weight and space are limited. Reconfigurable antennas save weight, space and money.

Four novel reconfigurable antenna elements were designed to work in the transition period where wireless communication shifts to the 5.7 GHz band: the reconfigurable Yagi, the reconfigurable corner-fed equilateral triangular loop antenna, the center-fed equilateral triangle antenna and the reconfigurable rectangular-spiral antenna. None of these antennas were reported before in the literature. Simulation results for all four antennas were obtained using IE3D. The reconfigurable Yagi antenna has a 3db beamwidth of 57.6^0 and a directivity of 8.62 db at the 2.45GHz frequency. At 5.78 GHz the antenna has a 3db beamwidth of 37.4^0 and a directivity of 11.49 db. The reconfigurable Yagi dimensions are (60mm X 175.01mm). This antenna was fabricated and tested. The measured results agree well with simulated results.

The largest dimension for the two types of the reconfigurable equilateral triangular loop antennas is 40.8mm, which makes them more compact in size compared to the Yagi antenna and hence more suitable for a reconfigurable array configuration. For the corner fed triangular loop antenna the IE3D simulation results show that the 3dB beamwidth of the antenna is 78.6^0 at 2.4 GHz the directivity is 8.07 dB. At 5.78GHz the 3dB beamwidth is 94^0 and the directivity is 7.175 dB. The reconfigurable center-fed rectangular loop antenna has a 3dB beamwidth of 89.25^0 and directivity of 7.1274 dB at the 2.45 GHz operating frequency. For the 5.78GHz configuration it has 94.7^0 beamwidth and the directivity is 6.9 dB.

The reconfigurable rectangular-spiral antenna is the most compact in size of all four antennas. It is (20mm x 20mm) in size. At 2.45 GHz it has a 3dB beamwidth of 85.6^0 and directivity of 6.47 dB. At 5.78GHz, the 3dB beamwidth is 82.5^0 and the directivity is 7.16 dB.

Combining reconfigurability with adaptivity is still not reported in the literature. We introduced the first antenna array of its kind by using the novel reconfigurable elements designed in this work in an adaptive array. Through several examples it was shown that the reconfigurable and adaptive antenna arrays were successful in nulling the noise incident on the array from different directions at the two frequencies of operation.

Future Work

In this dissertation we mainly used the Least Mean Square algorithm for the adaptive processor. The LMS and other methods that depend on it involve time averages. Thus the filter depends on the number of samples used in the computation. The processor cannot handle non-stationary environments like blinking jammers and time-varying clutter noise due to multipath signals. To extend this work other adaptive algorithms need to be investigated to improve the performance of the adaptive processor.

In the reconfigurable antennas designed in this dissertation we assumed that the MEMS switches are ideal open /close switches. In future work the effect of MEMS switches characteristics and

speed of operation needs to be incorporated to study their effect on the overall performance of the reconfigurable antenna element and on the array. Eventually this effect should be included in the adaptive processor and the algorithm used.

LIST OF REFERENCES

1. P. W. Howells, *Explorations in fixed and adaptive resolution at GE and SURC*, IEEE AP-S Trans., vol.24, No.5 Sept 1976, pp 575-584
2. S.P. Applebaum, *Adaptive arrays*, IEEE Ap-S Trans.,vol24, No.5, Sept 1976 pp 585-598
3. B. Widrow et al, *Adaptive antenna systems*, Proceedings of the IEEE, vol. 55, Dec. 1967, pp. 2143-2159
4. L. J. Griffiths, *A simple adaptive algorithm for real-time processing in antenna arrays*, Proc. IEEE, vol. 57,Oct. 1969 pp. 1696-1704
5. O. L. Frost,III, *An algorithm for linearly constrained adaptive array processing*, Proc. IEEE, vol. 60, Aug. 1972, pp. 926-935
6. R. L. Riegler and R. T. Compton, Jr., *An adaptive array for interference rejection*, Proc. IEEE, vol61, June 1973.
7. C. L. Zham, *Application of adaptive arrays to suppress strong jammers in the presence of weak signals*, IEEE Trans. Aerosp.Electron. Syst., vol. AES-9, March 1973, pp. 260-271.
8. L.E. Brennan et al., *Control-loop noise in adaptive array antennas*, IEEE Trans. Aerosp. Electron. Syst., vol. AES-7, March 1971, pp 254-262
9. L. E. Brennan and I. S. Reed, *Effect of envelope limiting in adaptive array control loops*, IEEE Trans. Aerosp. Electron. Syst., vol. AES-7, July 1971, pp. 698-700

10. L. E. Brennan and I. S. Reed, *Theory of adaptive radar*, IEEE Trans. Aerosp. Electron. Syst., vol. AES-9, March !973, pp. 237-252

11. L. E. Brennan et al. , *Adaptive arrays in airborne MTI radar*, IEEE AP-S Trans., vol.24, No.5 Sept 1976, pp 607-615

12. B. Widrow and J. M. McCool, *Adaptive algorithms based on the Methods of steepest descent and random search*, IEEE AP-S Trans., vol.24, No.5 Sept 1976, pp 615-637

13. C. A. Baird and G. G. Rassweiler, *Adaptive sidelobe nulling using digitally controlled phase-shifters*, IEEE AP-S Trans., vol.24, No.5 Sept 1976, pp 638-649

14. S. P. Applebaum, *Adaptive arrays with main beam constraints*, IEEE AP-S Trans., vol.24, No.5 Sept 1976, pp 650-662

15. K. Tako et al., *An adaptive antenna array under directional constraint*, IEEE AP-S Trans., vol.24, No.5 Sept 1976, pp 662-669

16. W. D. White, *Cascade preprocessors for adaptive antennas*, IEEE AP-S Trans., vol.24, No.5 Sept 1976, pp 670-684

17. D. J. Chapman, *Partial adaptivity for the large array*, IEEE AP-S Trans., vol.24, No.5 Sept 1976, pp 685-696

18. R. T. Compton, *An experimental four-element adaptive array*, IEEE AP-S Trans., vol.24, No.5 Sept 1976, pp 697-706

19. L. J. Griffiths, *Time-domain adaptive beamforming of HF Backscatter radar signals*, IEEE AP-S Trans., vol.24, No.5 Sept 1976, pp 707-720.

20. T. W. Washburn and L. E. Sweeney, *An on-line adaptive beamforming capability for HF Backscatter radar*, IEEE AP-S Trans., vol.24, No.5 Sept 1976, pp 721-732

21. R. O. Schmidt, *Multiple emitter location and signal parameter estimation*, IEEE AP-S Trans., vol.34, No.3 March 1986, pp 276-280

22. R. O. Schmidt and R. E. Franks, *Multiple source DF signal processing: an experimental system*, IEEE AP-S Trans., vol.34, No.3 March 1986, pp 281-290

23. W. F. Gabriel, Using spectral estimation techniques in adaptive processing antenna systems, IEEE AP-S Trans., vol.34, No.3 March 1986, pp 291-300

24. I. J. Gupta and A. A. Ksienski, *Dependence of adaptive array performance on conventional array design*, IEEE AP-S Trans., vol. Ap-30, pp.549-553, July 1982.

25. I. J. Gupta and A. A. Ksienski, *Prediction of adaptive array performance*, IEEE Trans. Aerospace Electron. Syst., vol. AES-19, no. 3, pp. 380-388, May 1983

26. I. J. Gupta and A. A. Ksienski -, Effect of mutual coupling on the performance of adaptive arrays, IEEE AP-S Trans., vol. AP-31, No. 5, pp. 785-791 Sept. !983

27. R. S. Adve and T. K. Sarkar, Compensation for the effects of mutual coupling on direct data domain adaptive algorithms, IEEE AP-S Trans., vol. 48, no.1, pp.86-94, Jan. 2000

28. James H. Shaffner et al, *Reconfigurable Aperture Antenna Using RF MEMS Switches for Multi-Octave Tunability and Beam Steering*, IEEE AP-S International Symposium Digest , 2000 pp 321-324 ,vol 1

29. K.C. Gupta et al, *Design of Frequency-Reconfigurable Rectangular Slot Ring Antennas*, , IEEE AP-S International Symposium Digest 2000 pp.326

30. James C. Maloney et.al, *Switched Fragmented Aperture Antennas,* IEEE AP-S International Symposium Digest 2000 pp310-313.

31. A. Fathy et al, *Silicon Based Reconfigurable Antennas,* IEEE AP-S International Symposium Digest 2000 pp 325, vol1

32. Jung-Chih Chiao et al, *MEMS Reconfigurable Vee Antenna, IEEE* MTT-S Digest 1999 pp 1515-1518

33. Balasundram Elamaran et. al*, A Beam-Steerer Using Reconfigurable PBG Ground Plane*, , IEEE MTT-S Digest 2000 pp. 835-838

34. W. Weedon, W. Payne and G. Rebeiz, *MEMS-Switched reconfigurable antennas*, Proc. IEEE International Symp., 2001, pp. 654-657.

35. M. L. VanBlaricum, *A brief history of photonic antenna configuration, Microwave Photonics,* 2000 International Topical Meeting, pp. 9-12.

36. Elliot R. Brown, *On the Gain of a Reconfigurable-Aperture Antenna*, IEEE AP-S Trans., Vol. 49, No.10, October 2001 , pp.1357-1362

37. R. F. Harrington, *Field Computation by Moment Methods*. New York: IEEE PRESS 1983

38. C. A. Balanis, *Advanced Engineering Electromagnetics*. New York: Wiely, 1989.

39. R. Mittra, *Computer Techniques for Electromagnetics*. New York: Hemisphere Publishing Corporation, 1987.

40. R.S. Adve and T.K. Sarkar, " Elimination of the Effects of Mutual Coupling in an Adaptive Nulling System with a Look Direction Constraint, " *AP-S International Symp. Digest*. 1996 pp. 1164-1167.

41. R. J. Mailloux, *Phased Array Antenna Handbook*, Norwood, MA: Artech House 1994.

42. J. Sor, Y. Qian, T. Itoh, *Characterization of a multi-mode microstrip aperture for phased array applications*, IEEE MTT-S Digest, 2000, pp. 589-592

43. R. Simons, D. Chun and L. Katehi, *Reconfigureable array antenna using MEMS actuators*, Proc. IEEE International Symp., 2001.